Dissolved nutrient retention dynamics in river networks: A modeling investigation of transient flows and scale effects

Sheng Ye,[1] Timothy P. Covino,[2] Murugesu Sivapalan,[1,3] Nandita B. Basu,[4] Hong-Yi Li,[5] and Shao-Wen Wang[1,6]

Received 1 February 2011; revised 16 May 2012; accepted 21 May 2012; published 30 June 2012.

[1] We have used a dynamic hydrologic network model, coupled with a transient storage zone solute transport model, to simulate dissolved nutrient retention processes during transient flow events at the channel network scale. We explored several scenarios with a combination of rainfall variability, and biological and geomorphic characteristics of the catchment, to understand the dominant factors that control the transport of dissolved nutrients (e.g., nitrate) along channel networks. While much experimental work has focused on studying nutrient retention during base flow periods in headwater streams, our model-based theoretical analyses, for the given parameter combinations used, suggest that high-flow periods can contribute substantially to overall nutrient retention, and that bulk nutrient retention is greater in larger rivers compared to headwaters. The relative efficiencies of nutrient retention during high- and low-flow periods vary due to changes in the relative sizes of the main channel and transient storage zones, as well as due to differences in the relative strengths of the various nutrient retention mechanisms operating in both zones. Our results also indicate that nutrient retention efficiency at all spatial scales of observation has strong dependence on within-year variability of streamflow (e.g., frequency and duration of high and low flows), as well as on the relative magnitudes of the coefficients that govern biogeochemical uptake processes: the more variable the streamflow, the greater the export of nutrients. Despite limitations of the model parameterizations, our results suggest that increased attention must be paid to field observations of the interactions between process hydrology and nutrient transport and reaction processes at a range of scales to assist with extrapolation of understandings and estimates gained from site-specific studies to ungauged basins across gradients in climate, human impacts, and landscape characteristics.

Citation: Ye, S., T. P. Covino, M. Sivapalan, N. B. Basu, H.-Y. Li, and S.-W. Wang (2012), Dissolved nutrient retention dynamics in river networks: A modeling investigation of transient flows and scale effects, *Water Resour. Res.*, *48*, W00J17, doi:10.1029/2011WR010508.

1. Introduction

[2] The phenomenon of oxygen depletion, or "hypoxia," in receiving waters such as lakes, estuaries, and coastal areas is now a worldwide environmental problem. This is partially caused by excess nutrient loading from terrestrial landscapes to aquatic environments that stimulates phytoplankton growth, the decomposition of which leads to depletion of dissolved oxygen. A large hypoxic zone occurs periodically in the northern Gulf of Mexico, where aquatic life is under threat due to nutrient induced eutrophication [*Rabalais et al.*, 2002]. Over 98% of the total nitrogen and phosphorous loading to the Gulf of Mexico is sourced to the Mississippi and Atchafalaya Rivers [*Dunn*, 1996], much of which originates from fertilized agricultural lands in the Midwest region of the United States. With increased attention to the eutrophication problems in the Gulf of Mexico and the greater Mississippi River Basin, there has been considerable emphasis given to quantifying the sources of nutrients, and the processes associated with the uptake, retention, and/or removal of nutrients within the watersheds and subwatersheds [*Bencala and Walters*, 1983; *Dodds et al.*, 2002; *Donner et al.*, 2002; *Mulholland et al.*, 2002; *Alexander et al.*, 2009; *Claessens and Tague*, 2009; *Claessens et al.*, 2009]. To avoid the confusion it might cause, in this paper we define nutrient retention as the temporary storage of nutrients in biomass (i.e., uptake)

[1]Department of Geography, University of Illinois at Urbana-Champaign, Urbana, Illinois, USA.
[2]Department of Land Resources and Environmental Sciences, Montana State University, Bozeman, Montana, USA.
[3]Department of Civil and Environmental Engineering, University of Illinois at Urbana-Champaign, Urbana, Illinois, USA.
[4]Department of Civil and Environmental Engineering, University of Iowa, Iowa City, Iowa, USA.
[5]Hydrology Technical Group, Pacific Northwest National Laboratory, Richland, Washington, USA.
[6]National Center for Supercomputing Applications, University of Illinois at Urbana-Champaign, Urbana, Illinois, USA.

Corresponding author: M. Sivapalan, Department of Civil and Environmental Engineering, University of Illinois at Urbana-Champaign, Urbana, IL 61801, USA. (sivapala@illinois.edu)

0043-1397/12/2011WR010508

and removal as the permanent loss of nutrient from the system (i.e., denitrification). We acknowledge that this retention is not necessarily equal to net loss from the stream system because it does not include contributions from remineralization [*Brookshire et al.*, 2009] or groundwater recharge [*Covino et al.*, 2010b]. Brookshire has found that during base flow periods streams could maintain steady state with equivalent nutrient loss by retention and gain from remineralization and groundwater inputs. However, in the absence of adequate information or data (e.g., denitrification rate, mineralization rate, groundwater concentration) to constrain a more complex representation of the nutrient cycle (e.g., including uptake, denitrification, mineralization), in this paper we limit our model to account for gross retention of inorganic nitrogen. More complex representations that incorporate various components of the nutrient cycle, transport of particulate organic nitrogen, and transport of other nutrients could be accounted for in our model given adequate process parameterizations or field-based evidence to constrain these additional aspects of stream biogeochemistry.

[3] The study of nutrient retention and removal processes within large watersheds can be organized into two distinct, but interacting, components: (1) the terrestrial landscape and (2) river networks, which are reactive pathways that connect the outputs of terrestrial systems to receiving waters. Both components involve interactions of flow (hydrological) processes with biogeochemical, geomorphological, and ecological processes on land and in the river network, all of which exhibit considerable heterogeneity and process complexity. In order to understand these processes and to use such understanding for management, we need predictive tools (i.e., models) that are based on fundamental theories of flow, transport, and reaction across the landscape and in the river network. This paper is aimed at describing the processes and interactions occurring exclusively within the river network and for this reason many details of landscape (hillslope) processes are left out. Previously there have been several watershed modeling studies that have focused on landscape (hillslope) biogeochemical scale processes [*Viney et al.*, 2000; *Li et al.*, 2010]. The work presented here focuses on dissolved nutrients, e.g., nitrate; however, the model can easily be further adapted to handle other solutes. The accompanying papers in this special section by *Harman et al.* [2011], *Thompson et al.* [2011], *Guan et al.* [2011], and *Basu et al.* [2011] address separately the transport and biogeochemical transformations in several components of the landscape and stream network, such as in the vadose zone, individual stream reaches, and in small watersheds. Furthermore, the paper by *Basu et al.* [2011] specifically addresses the effects of intra-annual streamflow variability on nitrate retention at the watershed scale, using a stochastic modeling approach.

[4] The theory of "nutrient spiraling" [*Webster and Patten*, 1979; *Newbold et al.*, 1982] serves as the foundation for much of the experimental and modeling work being carried out in the area of dissolved nutrient transport in river networks. It describes the coupled hydrological (e.g., advection) and biogeochemical (e.g., uptake) processes that control downstream nutrient transport and the cycling, or "spiraling," of nutrients between inorganic and organic forms [*Newbold et al.*, 1982]. *Bencala and Walters* [1983] proposed the "transient storage" model, which separates the river channel into two interacting compartments: the flowing water column or "main channel" (MC) zone and a more stagnant "transient storage" (TS) zone. The TS zone is a general term that represents any flow path where the velocity is much smaller than that in the MC. Examples include surface water "dead zones" such as pools, off-channel storages such as floodplains, the hyporheic zone, and other flow nonuniformities where the velocity is much smaller than that in the MC [*Stofleth et al.*, 2008; *Stewart et al.*, 2011]. Bencala and Walters' TS model is the basis for the now widely used one-dimensional transport model with inflow and transient storage (OTIS) [*Runkel*, 1998]. The OTIS model uses coupled partial differential equations in time and space (downstream distance) to characterize nutrient transport and transformation in rivers; it can consider transport and retention from both the MC and TS zones, including exchanges between the two. The model is also widely used, in combination with field measurements of solute concentrations and loads, to characterize reach-scale hydrologic and biogeochemical processes and their parameterizations [*Runkel*, 2007; *Böhlke et al.*, 2009].

[5] The mean distance a nutrient travels downstream before being taken up is defined as the uptake length S_W [L] [*Newbold et al.*, 1982]. The traditional approach to estimating S_W is to perform isotopic tracer or nutrient addition experiments within a stream reach and then plot the decline in nutrient concentration against downstream distance—the negative inverse of the slope (e.g., regression line) of this decline is S_W [*Stream Solute Workshop*, 1990; *Payn et al.*, 2008; *Böhlke et al.*, 2009; *Hall et al.*, 1998, 2009a]. Since S_W is related to hydrologic characteristics (e.g., velocity, depth), an uptake velocity defined as $v_f = (Q/w)/S_W$ (where Q [L^3 T^{-1}] is stream discharge and w [L] is wetted stream width), which partially accounts for hydrologic influences, is often computed to compare streams of different sizes and flow states [*Stream Solute Workshop*, 1990]. Accordingly, uptake velocity v_f [L/T] reflects biological demand relative to available nutrient concentration [*Wollheim et al.*, 2006].

[6] Previous studies have suggested that transient storage zones play an important role in nutrient retention within river channels [*Runkel and Bencala*, 1995]. They can act as a sink at the beginning of tracer injection experiments and as a source after injection is completed [*Bencala and Walters*, 1983]. It has been hypothesized that an increase in A_{TS}/A_{MC}, the ratio of the cross-sectional area of the TS zone (A_{TS}) to the cross-sectional area of the MC zone (A_{MC}) can promote nutrient uptake [*Bencala and Walters*, 1983; *Mulholland and De Angelis 2000*; *Paul and Hall*, 2002]. However, there have been several studies that cast doubt on the existence and possible effects of these linkages [*Hall et al.*, 2002; *Ensign and Doyle*, 2006]. Further work is still needed, at a range of scales, to understand and clarify the relative contributions of retention mechanisms in MC and TS zones.

[7] A majority of nutrient release experiments have been carried out in small headwater streams [*Tank et al.*, 2008] during low-flow conditions [*Hall et al.*, 2009b], which may represent times and conditions of high nutrient retention [*Peterson et al.*, 2001; *Böhlke et al.*, 2009]. Nutrient release experiments are typically more tractable in small

headwater streams than in larger rivers or during times of high discharge [*Hall and Tank*, 2003; *Hall et al.*, 2009b]. However, *Hall et al.*'s [2009b] work in a mountain stream suggested that biological demand for nitrate was much higher than expected during floods and that reach scale nutrient uptake during low flows and spring floods were similar. This can potentially be attributed to the presence of a large hyporheic zone (i.e., increased extent of the hyporheic zone during flood events) relative to the size of the drainage area. Furthermore, recent modeling studies have indicated that in spite of the low efficiency of retention and removal per unit length, larger rivers, with associated longer travel times and larger mass input, can have significant contributions to transport of nutrients throughout the overall network in spite of lower nutrient retention efficiencies [*Wollheim et al.*, 2006; *Ensign and Doyle*, 2006], the reasons for which are not fully clear. Combined, these results suggest that it is important to understand nutrient retention processes across a range of flow states and stream sizes.

[8] Characterization of biogeochemical processes in streams is typically accomplished through a combination of field experiments and process models [*Bencala and Walters*, 1983; *Runkel*, 1998; *Claessens and Tague*, 2009; *Claessens et al.*, 2009; *Covino et al.*, 2010a]. The results of these field experiments are used to estimate model parameters and to understand the factors affecting nutrient transport at the reach scale. To understand how nutrient transport processes evolve in the downstream direction, and how they impact the dynamics in larger rivers, we need watershed network scale models that can accommodate terrestrial loading, transport, and transformation along the river channel network. There are several biogeochemical models that are in wide use to predict nutrient transport at different spatial scales [e.g., *Smith et al.*, 1997; *Donner et al.*, 2002; *Mulholland et al.*, 2002, 2008; *Seitzinger et al.*, 2002, *Wollheim et al.*, 2006, 2008; *Alexander et al.*, 2009]. Many of these models use observed data to predict nutrient transport as a function of hydrologic variables (i.e., stream depth, travel time). These empirical relationships are then applied at the catchment scale, to obtain annual estimates of nutrient export [*Smith et al.*, 1997; *Goolsby et al.*, 2000]. Other models have applied the one-dimensional advection-dispersion equation to capture reach scale nutrient cycling processes for each month, and have expressed bulk retention k_e as a function of nutrient concentration, flow depth, and water temperature [e.g., *Alexander et al.*, 2009]. Many of these models have assumed steady flow conditions, and although they capture the impact of seasonal variability on nutrient transport, they are unable to make predictions under highly variable flow conditions that occur during flood events, as well as seasonally over the year, or in space (e.g., across the river network), a notable exception being the work by *Wollheim et al.* [2008]. The work presented in this paper specifically addresses the problem of characterizing the likely impacts of variable flow dynamics (within-event as well as inter-event) on nutrient retention and export processes, and associated scale effects.

[9] Every watershed possesses unique hydrological, biological, and geomorphic characteristics. These factors, which partially control nutrient transport, may vary both within watersheds, as well as between watersheds. Without a more complete understanding of the process controls on nutrient transport and transformation and their variability across spatial and temporal scales, it is difficult to develop generalized models and predictions. Furthermore, field experiments have produced contradictory results, and the existence of relationships between the size of the TS zone and nutrient uptake remain inconclusive [e.g., *Marti et al.*, 1997; *Ensign and Doyle*, 2006]. This is partially due to uncertainty regarding retention and/or removal rates in the MC and TS zones, knowledge of the relative sizes of the TS and MC zones, and consequently the relative contributions from the two zones that combine to produce bulk nutrient retention. Lack of resolution of these questions will have significant impact on our ability to predict nutrient transport at the watershed scale. For example, moving in the downstream direction in a river network, nutrient retention may: be reduced by the increase of both flow depth and flow velocity; potentially increase due to increasing A_{TS}/A_{MC} ratio accompanying the increase in stream size; or remain constant due to the compensating effects of the above two factors.

[10] To address these questions, a comprehensive numerical framework that can accommodate the impact of various process controls (i.e., hydrology, biogeochemistry, and geomorphology) on nutrient transport within watersheds is needed. Ideally, models of nutrient transport processes at the network scale must be consistent with more widely accepted process representations, such as those represented in the OTIS model, and with field observations. This has been the motivation for the modeling study presented here. A recent review by *Helton et al.* [2011] has highlighted major weaknesses in the current generation of nitrogen cycling models in river networks in that they: oversimplify catchment hydrology; oversimplify network hydrogeomorphology; incorporate unidirectional uptake of nitrogen rather than cycling in the context of other elements (i.e., stoichiometric constraints); and focus on base flow or annual mean conditions, ignoring the ecological relevance of seasonal cycles and faster temporal dynamics.

[11] This paper focuses on the last of these, namely, the influence of temporally dynamic hydrology on nutrient export, and particularly we distinguish between retention during high-flow and low-flow periods; determine the relative contributions of the TS and MC zones to retention; and investigate the roles of hydrologic variability (as governed by climate and landscape filtering), network geomorphology, and scaling these dynamics across space and time. We implement a coupled hydrological-solute-transport model to address the following questions:

[12] (1) How much nutrient retention occurs during low-flow periods versus during high-flow periods, and what are the contributions to retention from the main channel (MC) and the transient storage (TS) zones?

[13] (2) What are the impacts of within-year streamflow variability on the fraction of nitrate removed and delivered at the watershed scales?

[14] (3) How are the answers to the two questions posed above influenced by scale effects (i.e., size of river or contributing watershed area), including how retention rates and their process controls change as one moves from the reach scale to the network scale?

[15] Through implementation of the model across the river network of a ~500 km^2 watershed we seek to elucidate

watershed scale biogeochemical and hydrological responses, as different from reach scale process representations, and to understand how hydrologic variability interacts with network structure and patterns of hydraulic geometry and solute transport processes, giving rise to these newly emergent properties.

2. Methodology

[16] The modeling framework we use here combines a dynamic flow model in a river network, based on the representative elementary watershed (REW) theory of *Reggiani et al.* [1998, 1999, 2001], with a network nutrient transport and retention model based on upscaling of the OTIS model equations for dissolved nutrients [*Bencala and Walters*, 1983; *Runkel*, 1998], with explicit inclusion of the interactions between the MC and TS zones. The focus of the present paper is on the network nitrate (NO_3-N) retention processes; for this reason hillslope processes are somewhat oversimplified and hillslope flow response is simulated with a linear bucket model with an assumed mean residence time. NO_3-N concentrations of hillslope flows are assumed constant in time and space, and yet, since discharge is highly variable, the nitrate load is variable as well. The details of each of the model components are given in Figure 1. More advanced versions of these components are elaborated upon in the accompanying papers by *Harman et al.* [2011], *Thompson et al.* [2011], and *Guan et al.* [2011].

2.1. Study Area

[17] The nominal study area is the Little Vermilion River watershed (Figure 2) and the river network is extracted from a DEM for this watershed. This watershed drains a 489 km^2 area across three counties, Vermilion, Champaign, and Edgar, and is generally flat with a slope of 1% or less [*Mitchell et al.*, 2000; *Algoazany*, 2006]. It is a typical agricultural watershed in east-central Illinois that is drained by an extensive network of tile drains. The land use in Little Vermilion is quite intensive. Nearly 90% of the area is planted with a rotation of corn and soybean crops. The dominant soil type in this watershed is silty loam and silty clay loam, with low hydraulic conductivity values.

2.2. Network Hydrologic Model

[18] The network flow model, based on the REW approach, builds on the balance equations for mass and momentum for a hierarchical river network derived by *Reggiani et al.* [2001]. The REW approach disaggregates the whole watershed into a number of subwatersheds (REWs), with the REWs being considered the smallest functional units of the model, with each REW having only one stream reach and being linked to all other REWs via the river network. *Tian* [2006] developed a numerical model, THREW (Tsing Hua representative elementary watershed), based on a set of ordinary differential equations (ODEs) of the coupled mass and momentum balance equations at the REW scale [*Li and Sivapalan*, 2011], including extensions to incorporate explicit formulations for energy balance applicable to cold regions [*Tian et al.*, 2006].

[19] Since our objective is to explore process controls on nitrate transport in a river network only, we use a simplified version of THREW, where each REW is divided into two subregions only: a hillslope region and a channel region

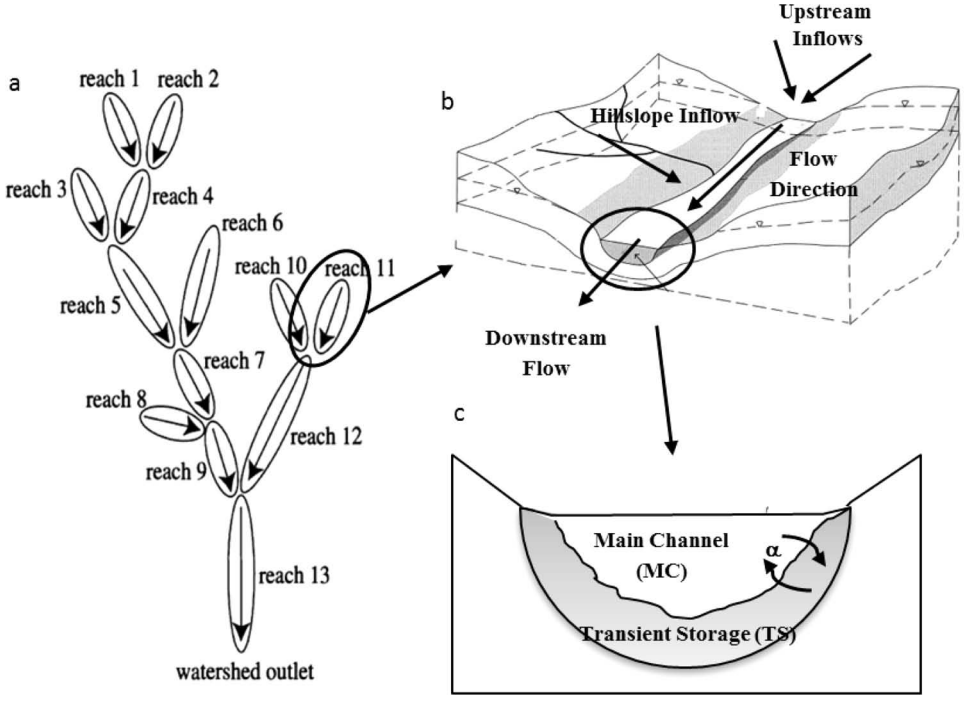

Figure 1. Schematic of the coupled hydrological-solute-transport model: (a) Watershed discretization into several REWs organized around the river network; (b) each REW includes a hillslope (landscape element) and a channel reach; and (c) two-zone solute transport model that includes the main channel (MC) zone and a transient storage (TS) zone; α is a coefficient that governs nutrient exchange between the MC and TS zones.

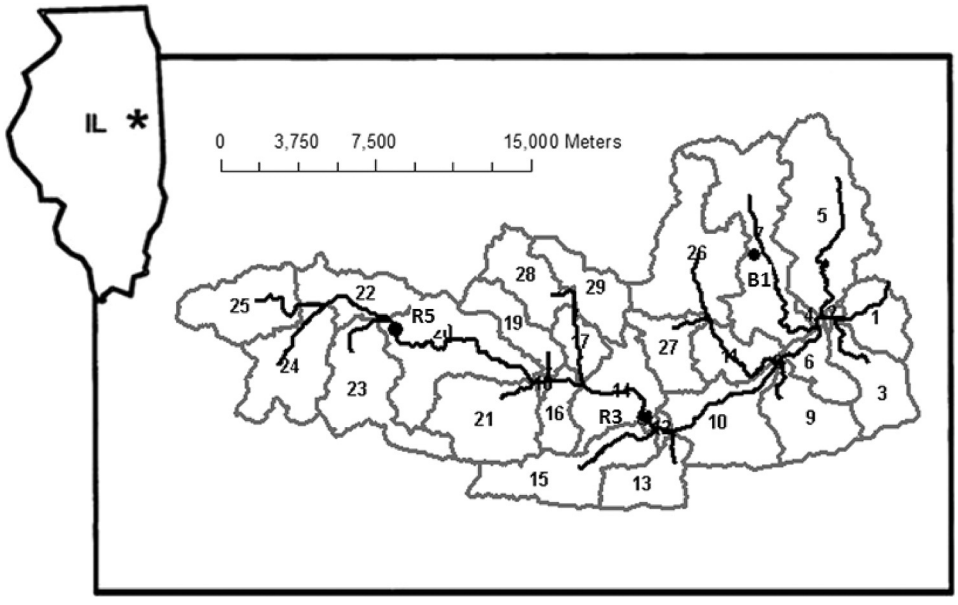

Figure 2. Map of the study area, Little Vermilion Basin in east-central Illinois, including the delineation of 29 REW boundaries. Bold line is the river network.

(Figure 1). We use a simple lumped bucket model to represent the hillslope response to precipitation for REW$_i$:

$$\frac{dS_h^i}{dt} = PA^i - Q_h^i - ET^i, \tag{1}$$

$$Q_h^i = \frac{S_h^i}{\tau_h}, \tag{2}$$

$$ET^i = \frac{S_h^i}{\tau_e}, \tag{3}$$

where S_h^i is water storage of REW$_i$ in the hillslope [L^3], P is the rainfall intensity [$L\ T^{-1}$] and is assumed uniform across the watershed, A^i is the area of REW$_i$ [L^2], Q_h^i is flow that enters the channel network directly from the local hillslope area [$L^3\ T^{-1}$], τ_h is the mean residence time with respect to subsurface flow [T], ET^i is the evaporation [$L^3\ T^{-1}$], and τ_e is mean residence time with respect to evapotranspiration [T]. The presence of an extensive network of tile drains leads to the dominance of subsurface drainage while surface runoff is rare [*Li et al.*, 2010]. These considerations justify the use of simple conceptual models of the hillslope hydrologic response [*Basu et al.*, 2009], such as the one adopted here.

[20] The water balance equation for the river reach i (associated with REW$_i$), with inflows from the hillslope and two upstream nodes, can be written as follows:

$$\frac{dS_{\mathrm{MC}}^i}{dt} = Q_h^i + \sum \mathrm{Q}_{\mathrm{up}}^j - Q_{\mathrm{out}}^i, \tag{4}$$

$$Q_{\mathrm{out}}^i = v^i A_{\mathrm{MC}}^i, \tag{5a}$$

$$Q_{\mathrm{up}}^j = v^j A_{\mathrm{MC}}^j, \tag{5b}$$

where S_{MC}^i is water storage at local reach i [L^3], Q_{up}^i is the inflow from upstream nodes (in a bifurcating network we assume there are at most two upstream reaches) [$L^3\ T^{-1}$], v^j is the velocity at upstream end, for reach j [$L\ T^{-1}$], A_{MC}^j is estimated at the beginning of any time step by dividing the water storage (S_{MC}^i is cross-sectional area of the jth upstream reach [L^2], Q_{out}^i is the outflow from reach i [$L^3\ T^{-1}$], and v^i is the velocity at local reach i [$L\ T^{-1}$].

[21] The channel cross-sectional area A_{MC}^i is estimated at the beginning of any time step by dividing the water storage (S_{MC}^i) at the end of previous time step by the channel reach length (L^i), while the velocity v^i is estimated through recourse to a reach scale momentum balance equation (i.e., Saint-Venant momentum balance equation).

$$\underbrace{\rho A_{\mathrm{MC}}^i L^i \frac{d}{dt} v^i}_{\text{Inertia}} = \underbrace{\rho g A_{\mathrm{MC}}^i L^i \sin\gamma^i}_{\text{Gravity}} - \underbrace{\frac{1}{8}\rho P^i L^i \zeta^i v^i |v^i|}_{\text{Chezy resistance}} \pm \underbrace{\sum_{j\neq i} \frac{1}{4}\rho g h^i (A_{\mathrm{MC}}^i + A_{\mathrm{MC}}^j)\cos\delta^{ij}}_{\text{Pressure forces exchanged across end sections}} - \underbrace{\frac{1}{2}\rho g h^i A_{\mathrm{MC}}^i}_{\text{Pressure forces at watershed outlet}}, \tag{6}$$

where ρ is the density of water [$M\ T^{-3}$], A_{MC}^i is the cross-sectional area in an upstream or downstream reach j [L^2], L^i is reach length of REW$_i$ [L], g is gravitational acceleration [$L\ T^{-2}$], $\sin\gamma^i$ is the mean slope of REW$_i$, P^i is average wetted perimeter of local REW$_i$ [L], h^i is the mean depth of REW$_i$ [L], ζ^i is the Darcy-Weisbach friction coefficient ($\zeta^i = 8g\,(n^i)^2 (R^i)^{-1/3}$, n^i is a roughness coefficient, and R^i is the hydraulic radius), and δ^{ij} is the angle of confluence of upstream reach j and local reach i. In equation (6), when reach j is upstream of reach i, the sign in front of the pressure force term is generally + and is – when reach j is downstream of reach i. The last item in equation (6) will remain only if the local reach is directly upstream of the outlet. As the influence of the confluence angle on the resulting velocity is very small, we assume it is equal to 1 (unity) and

remove it without loss of accuracy. In this paper, for simplicity we ignore the inertia term in the momentum equation and we obtain the simplified equation for velocity as follows:

$$v^i = \frac{1}{n^i}\sqrt{\frac{(R^i)^{1/3}}{P^i L^i}\left(A^i_{\mathrm{MC}} L^i \sin\gamma^i \pm \sum_{j\neq i}\frac{1}{4}h^i(A^i_{\mathrm{MC}} + A^j_{\mathrm{MC}}) - \frac{1}{2}h^i A^i_{\mathrm{MC}}\right)}. \tag{7}$$

2.3. Specification of Hydraulic Geometry

[22] The size of the TS zone is directly related to the wetted perimeter of the channel, and so to accurately simulate the retention rate in TS, it is necessary to adequately represent the hydraulic geometry of the channel. The hydraulic geometry is also crucial to capture the space-time variations of flow velocity that ultimately determines the water residence time in the river reaches. An extensive survey of at-a-site and downstream hydraulic geometry has been carried out for Illinois streams by *Stall and Fok* [1968]. They obtained best fits between measured top width, flow depth, velocity, and cross-sectional area as power functions of flow frequency and drainage area for several streams in Illinois. The relations for top width and flow depth extracted from the results of *Stall and Fok* [1968] are as follows:

$$\ln w^i_{\mathrm{top}} = -1.23 + 0.27\ln A^i_{\mathrm{MC}} + 0.18\ln A^i_d, \tag{8a}$$

$$\ln h^i_{\mathrm{MC}} = 1.23 + 0.73\ln A^i_{\mathrm{MC}} - 0.18\ln A^i_d, \tag{8b}$$

where w^i_{top} is the top width of reach i [L], h^i_{MC} is the mean depth of reach i [L], A^i_{MC} is the cross-sectional area of reach i [L^2], and A^i_d is the total contributing (drainage) area for the outlet at reach I [L^2]. We use these regionalized equations to construct the hydraulic geometry across the network of the Little Vermilion River watershed. Previous versions of the THREW model assumed the channel cross-sectional area to be rectangular [*Tian*, 2006; *Li et al.*, 2010; *Li and Sivapalan*, 2011]. In this paper, in order to better characterize the wetted perimeter and channel flow velocity and solute transformations, especially under low-flow conditions, the cross section was changed from rectangular to trapezoidal. Model predicted magnitudes of flow velocity, both at-a-site and downstream, were tested and successfully verified against the corresponding regionalized estimates of *Stall and Fok* [1968] (not included here for reasons of brevity).

2.4. Network Model of Solute Transport

[23] The solute transport model is derived from the one-dimensional transport with inflow and storage model (OTIS) applicable to a single reach [*Bencala and Walters*, 1983; *Runkel*, 1998].

$$\frac{\partial C_{\mathrm{MC}}}{\partial t} = \underbrace{-\frac{Q}{A_{\mathrm{MC}}}\frac{\partial C_{\mathrm{MC}}}{\partial x}}_{\text{Advection}} + \underbrace{\frac{1}{A_{\mathrm{MC}}}\frac{\partial}{\partial x}\left(A_{\mathrm{MC}} D \frac{\partial C_{\mathrm{MC}}}{\partial x}\right)}_{\text{Dispersion}} + \underbrace{\frac{q_L}{A_{\mathrm{MC}}}(C_L - C_{\mathrm{MC}})}_{\text{Lateral flux}} + \underbrace{\alpha(C_{\mathrm{TS}} - C_{\mathrm{MC}})}_{\text{Nutrient exchange}} - \underbrace{k_c C_{\mathrm{MC}}}_{\text{Uptake from MC}}, \tag{9a}$$

$$\frac{dC_{\mathrm{TS}}}{dt} = \underbrace{\alpha\frac{A_{\mathrm{MC}}}{A_{\mathrm{TS}}}(C_{\mathrm{MC}} - C_{\mathrm{TS}})}_{\text{Nutrient exchange}} - \underbrace{k_s C_{\mathrm{TS}}}_{\text{Uptake from TS}}, \tag{9b}$$

where C_{MC} is nitrate concentration within the MC [$M\,L^{-3}$], C_{TS} is concentration within the transient storage zone [$M\,L^{-3}$], C_L is the concentration of lateral inflow [$M\,L^{-3}$], A_{MC} is the cross-section area of MC [L^2], A_{TS} is the cross-section area of the TS zone [L^2], x is longitudinal distance [L], D is dispersion coefficient [$L^2\ T^{-1}$], α is the exchange rate between the main channel and transient storage [T^{-1}], q_L is lateral inflow rate [$L^3\ T^{-1}\ L^{-1}$], and k_c and k_s are the uptake rate coefficients for reactive solutes from the MC and the TS zones, respectively [T^{-1}]. This model considers nutrient advection and dispersion in the MC, but in the TS zone solutes are assumed well mixed and the flow velocity is slow enough not to account for flows in the longitudinal direction. The nutrient exchanges between the MC and TS zones are assumed to be proportional to the concentration gradient between the two compartments.

[24] In the current study we seek to investigate nutrient transport at the network scale, across stream types and sizes, and during both low-flow and high-flow periods. Accordingly, we upscale the above model to the network scale, assuming that the effects of hydrodynamic dispersion are small and negligible compared to network dispersion (also known as geomorphologic dispersion) (see *Robinson et al.* [1995] for a justification of this assumption), and the nutrient retention in the MC zone is a function of water storage and the average of the upstream inflow concentrations and the local concentration. Upscaling of the OTIS biogeochemistry equations (equations (9a) and (9b)) to the network scale then leads to the following two coupled governing equations for a stream reach belonging to REW_i (each reach is considered as individual segment to which equations (9a) and (9b) are applied):

$$\frac{d(S^i_{\mathrm{MC}} C^i_{\mathrm{MC}})}{dt} = \underbrace{Q^i_h C^i_h}_{\text{Hillslope input}} + \underbrace{\sum(Q^j_{\mathrm{up}} C^j_{\mathrm{MC}})}_{\text{Upstream inputs}} - \underbrace{Q_{\mathrm{out}}{}^i C^i_{\mathrm{MC}}}_{\text{Output}} - \underbrace{\alpha S^i_{\mathrm{MC}}(C^i_{\mathrm{MC}} - C^i_{\mathrm{TS}})}_{\text{Nutrient exchange}} - \underbrace{k_c\frac{(C^i_{\mathrm{MC}} + \sum C^j_{\mathrm{MC}}/2)}{2} S^i_{\mathrm{MC}}}_{\text{Water Column \& Benthic Uptake}}, \tag{10a}$$

$$\frac{d(S^i_{\mathrm{TS}} C^i_{\mathrm{TS}})}{dt} = \underbrace{\alpha\frac{A_{\mathrm{MC}}}{A_{\mathrm{TS}}} S^i_{\mathrm{TS}}(C^i_{\mathrm{MC}} - C^i_{\mathrm{TS}})}_{\text{Nutrient exchange}} - \underbrace{k_s C^i_{\mathrm{TS}} S^i_{\mathrm{TS}}}_{\text{Uptake from TS}}, \tag{10b}$$

where C^i_{MC} is the concentration in the local channel [$M\,L^{-3}$], C^i_{TS} is the concentration within the transient storage zone [$M\,L^{-3}$], C^j_{MC} is the concentration in the upstream reach j [$M\ L^{-3}$], α is the exchange rate between the MC and TS zones [T^{-1}], S^i_{TS} is the volume of water in the TS zone [L^3] ($S^i_{\mathrm{TS}} = L^i\ P^i\ h^i_{\mathrm{TS}}$, L^i is the length of the reach, P^i is the wetted perimeter, and h^i_{TS} is the depth of TS zone, which is assumed constant), and k_s is the uptake rate coefficient from TS zone [T^{-1}].

[25] In this paper the model is implemented with k_c assumed to vary with flow depth, as $k_c = v_c/h$ (where v_c is

the uptake velocity in MC [$L\ T^{-1}$], in analogy with the relationship often assumed between the first order retention rate and uptake velocity of the *combined system*: $k_e = v_f/h$). In the base experiment, decreasing k_c as a function of flow depth h assumes that uptake/removal on benthic biofilms dominates MC retention. There is a possibility that pelagic uptake could increase in the downstream direction, in which case the k_c would not decrease with increasing depth; however in the absence of empirical evidence on pelagic uptake, we decided not to include this scenario here. Detailed theoretical and field investigations to quantify this impact could be important for future study. The uptake velocity in MC (v_c) and uptake coefficient in TS (k_s) are assumed to follow first order kinetics [as in *Wollheim et al.*, 2006]. Since the goal here is to examine the impact of hydrologic variability on nutrient retention and because limited data are available for the scaling of MC and TS uptake metrics from headwater to higher order reaches v_c and k_s are set at constant values across the watershed. As data evidence and process formulations advance, these aspects can be improved in subsequent versions of the model.

2.5. Climate and Nitrate Inputs

[26] In the research that is reported in this paper, the coupled model is driven by stochastic precipitation inputs that are generated by a stochastic event rainfall model developed by *Robinson and Sivapalan* [1997]. In order to explore the effects of flow variability on net retention, we constructed three different rainfall scenarios (consisting of 10-year long synthetic time series), and simulated the coupled hydrological and nutrient transport processes within the stream network under each scenario. For illustration we have denoted these as climates 1, 2, and 3: climate 1 (low variability), climate 2 (intermediate), and climate 3 (high variability). The rainfall series are a function of storm duration t_r, interstorm period t_b, and mean rainfall intensity p. The storm duration t_r and interstorm period t_b are assumed to follow exponential probability density distributions, and their mean values vary sinusoidally with time of year ($t = T + A\sin[2\pi/(\xi - \xi_r)/\omega]$, where t represents the mean value for the exponential distribution (for t_r or t_b) for a given time period within the year, T is the corresponding annual average value (annual mean of t_r, t_b), A is the amplitude of the seasonal variation, ω is the total number of time units in a year (here 8760 h per year), ξ is the time within the year, and ξ_r is the seasonal phase shift); the precipitation intensity (p) is statistically dependent on t_r, its conditional distribution (given t_r) follows a gamma distribution, as the parameters of this gamma distribution are also a function of t_r, the mean p of the gamma distribution also varies sinusoidally like t_r and t_b. All three climates share the same seasonality (the amplitude A and the phase shift x_r), in which rainfall occurs during the spring and fall seasons and similar annual precipitation (~1000 mm per year) but distinct annually averaged storm duration t_r, interstorm period t_b, and rainfall density p. The details of the model are given by *Robinson and Sivapalan* [1997].

[27] The annual mean value of these characteristics of rainfall inputs are presented in Table 1 for the three climates. There has been no attempt to match any of these climatic inputs, including annual rainfall and potential evaporation totals, their intra-annual variability, and the statistical characteristics of storm events to climatic conditions prevailing in the Little Vermilion River watershed. All simulations used a hillslope residence time τ_h of 100 h, and evaporation time scale τ_e of 100 h. Figure 3 presents, as illustration, the time series of precipitation inputs for climate 2. Except when the focus of the analysis is on comparisons between different climate scenarios, most of the results presented in subsequent sections relate to climate 2, with the mean annual water balances as follows: $ET/P = 0.50$, $Q/P = 0.50$, $Q_b/Q = 0.22$ (P, ET, Q, and Q_b are, respectively, annual precipitation, evaporation, total runoff, and base flow). These are not meant to be exact reproductions of the water balance of the Little Vermilion River watershed; nevertheless, they are representative of well-drained agricultural basins in much of the Midwestern United States.

[28] Nitrate concentrations of hillslope contributions to the river channels are kept constant in space and time at a notional value of 15 mg NO_3-N/L during both flood events and base flow periods, which is the mean concentration of observed tile drain data in Little Vermilion watershed. Low temporal variability in nitrate concentrations relative to that of water discharge in intensively managed agricultural catchments (i.e., chemostatic export) has been discussed in recent papers [*Basu et al.*, 2010; *Thompson et al.*, 2011; *Guan et al.*, 2011]. Parameters associated with the solute transport processes within the coupled model are also assumed to remain constant in space and time. Our assumed first-order kinetic model precludes any dependence on background nitrate concentrations [*O'Brien et al.*, 2007; *Covino et al.*, 2010b]

Table 1. Effects of Hydrological Variability and Geomorphologic and Biogeochemical Factors on Nitrate Net Retention Rates During High and Low Flows

	Climate 1			Climate 2			Climate 3		
Mean t_r (h)	34			34			15		
Mean t_b (h)	76			186			227		
Mean p (mm h^{-1})	0.4			0.8			2.0		
Mean $CV(Q)$ of headwater streams	2.08			3.01			3.44		
$CV(Q)$ of outlet stream	2.01			2.92			3.32		
	Whole Year	During High Flows	During Low Flows	Whole Year	During High Flows	During Low Flows	Whole Year	During High Flows	During Low Flows
k_e When k_c decreases, TS depth constant (/h)	0.0135	0.012	0.0217	0.0116	0.0103	0.0185	0.0112	0.0101	0.0185
k_e When k_c decreases, TS depth increases downstream (/h)	0.0214	0.0202	0.0326	0.0179	0.017	0.0267	0.017	0.0163	0.0263

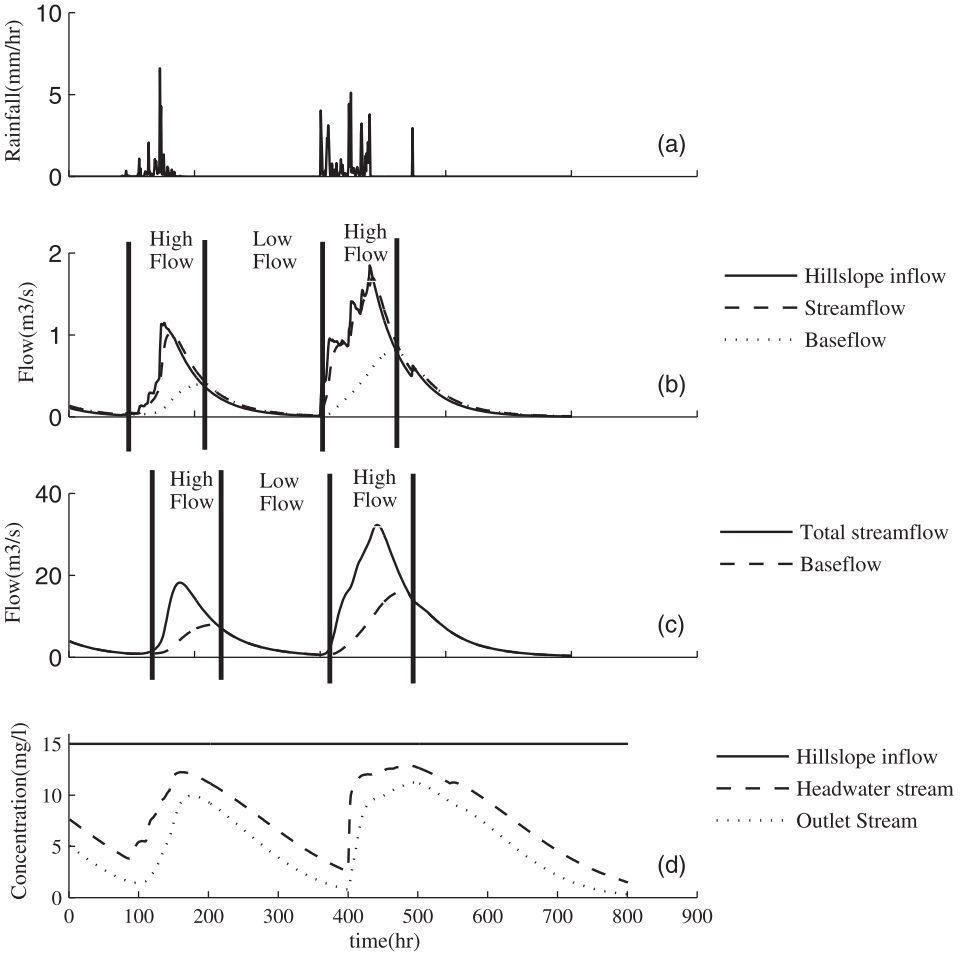

Figure 3. Schematic describing typical time series of rainfall, hillslope inflows and streamflows and nutrient concentrations for climate 2 (see Table 1): (a) rainfall event patterns: intensity = 0.8 mm h^{-1}, $t_r = 34$ h, $t_b = 186$ h; (b) hillslope inflows and streamflow for a headwater stream; (c) streamflow at the catchment outlet, and illustration of flow separation into high-flow and low-flow periods; and (d) nutrient concentration of hillslope input (assumed constant at 15 mg NO_3-N/L), and for a first order REW and at the catchment outlet.

and dependence on other environmental variables such as temperature are also ignored for the present. The parameter values are notional literature values chosen from a survey of field measurements, as shown in Table 2 [*Runkel*, 2000; *De Smedt et al.*, 2005; *Hall et al.*, 2009b; *Stewart et al.*, 2011]. Default values of the nutrient uptake parameters used in this study are: $v_c = 0.002$ m h^{-1}, $k_s = 0.2$ h^{-1}, and $\alpha = 0.1$ h^{-1}. According to *Stewart et al.* [2011] the ratio of the size of the hyporheic TS zone to that of MC is 0.35, which is an average value for the Ipswich River network in Massachusetts. In this paper, in the default case, the thickness of the TS zone is held constant throughout the network at a value of 0.06 m; for a typical first order reach this produces a mean $A_{TS}/A_{MC} = 0.35$, which is consistent with *Stewart et al.* [2011].

[29] In this paper we explore the effects of MC contributions as opposed to TS dominance of uptake and retention processes. As part of the sensitivity analysis presented later in the paper, we will also consider two scenarios in which MC and TS contributions are roughly equivalent and where the MC contribution is larger than TS through the use of larger v_c values and smaller k_s values. Each scenario is simulated for a 10-year period, and the initial nutrient

Table 2. The Literature Sources for the Parameter Values Chosen

Parameter	Value in Base Experiment	Sources
v_c	0.002 m h^{-1}	0.001–1.07 [*Hall et al.*, 2009a][a]
α	0.1/h	0.036–3.6 [*De Smedt et al.*, 2005]
k_s	0.2/h	0.01–7.2 [*Runkel*, 2000]
TS depth constant	Thickness = 0.06 m	makes $A_{TS}/A_{MC} \sim 0.35$ for a first order REW
TS Depth increases downstream	$A_{TS}/A_{MC} = 0.35$	[*Stewart et al.*, 2010]

[a]These only refer to the uptake velocity of the whole stream v_f; the range of values for v_c used in this paper are smaller.

storages in MC and TS are assumed to be zero (i.e., there is no nutrient stored at the beginning of the simulation). These sensitivity analyses are carried out to verify that the extent of emergent scaling effects extracted from the simulations are not fundamentally altered by the range of parameter values used here.

3. Results

[30] With the use of the coupled hydrological-solute-transport model we explore the richness of a variability of nutrient retention process in space and time. In the time domain we characterize the within-year variability by partitioning the year into event-driven high-flow and subsequent low-flow periods. In the space domain we partition the river reach into two zones: the main channel (MC) and the transient storage (TS). We begin the analysis in first order watersheds (REWs), and systematically extend the analysis of the above partitioning, in a nested manner, to all higher order watersheds, including the highest order watershed at the outlet.

[31] Figure 3 illustrates the manner in which we partition the year into high-flow and low-flow periods. It presents the synthetic time series of precipitation for climate 2, and the corresponding model predicted hillslope inflows (at a constant concentration of 15 mg L^{-1}), and streamflows and nitrate concentrations for a first order stream (REW 24), and for the stream at the watershed outlet. We use the base flow separation algorithm of *Lyne and Hollick* [1979] to partition the time series of flows in all river reaches, into separate event-associated high-flow periods, and subsequent low-flow periods, as shown in Figure 3. This allows us to estimate the magnitudes of nitrate loading (inputs), retention and export separately during event (high-flow), and inter-event (low-flow) periods, for all streams of all orders, and also at the watershed/network scale by aggregating the estimates for all streams that lie within each nested watershed. We repeat the same analyses to estimate the separate contributions to retention by the MC and TS zones. The results are presented next.

3.1. Breakdown Into High-Flow and Low-Flow Periods, and Between MC and TS Zones

[32] Figure 4 presents the partitioning of the total nitrate inputs between high-flow and low-flow periods (in this and all subsequent cases the results are annual averages based on 10-year long simulations). In the case of the MC zone, the inputs are loadings from the hillslopes. In the case of the TS zone the inputs are exchanges from the MC zone, which are governed by differences in nutrient concentrations between the two zones. Because the nutrient concentration of hillslope inflows is constant, loading into the MC during high flows is larger (~3 times) than during low-flow periods (Figure 4). Regardless of the simplifying assumption of constant concentration of hillslope inflows, the result in terms of loading is consistent with previous research that also has indicated large magnitudes of nutrient loading during high-flow periods [*Royer et al.*, 2006]. On the other hand, in the case of the TS the differences between high- and low-flow periods is much less since the effect of the concentration gradients is modulated by differences in residence time.

[33] We next present the corresponding results for bulk retention during high-flow and low-flow periods separately for the MC and TS zones, as well as for the combined system (see Figure 5). We define the fractional retention as the ratio of nitrate retained in a certain zone during a certain period versus the total retention that occurs in both MC and TS zones through the year. For example, $f_{h-\mathrm{MC}}$ is the percentage of nitrate retained in MC during high flow versus the total retention in both MC and TS zones annually. The calculation of the fractional retention during high-flow and low-flow periods is as follows:

$$f_{h-\mathrm{MC}} = \frac{\sum_i \int_{T_h} k_c C^i_{\mathrm{MC}}(t) S^i_{\mathrm{MC}}(t)\,dt}{\sum_i \int_T [k_c C^i_{\mathrm{MC}}(t) S^i_{\mathrm{MC}}(t) + k_s C^i_{\mathrm{TS}}(t) S^i_{\mathrm{TS}}(t)]\,dt}, \tag{11a}$$

$$f_{l-\mathrm{MC}} = \frac{\sum_i \int_{T_l} k_c C^i_{\mathrm{MC}}(t) S^i_{\mathrm{MC}}(t)\,dt}{\sum_i \int_T [k_c C^i_{\mathrm{MC}}(t) S^i_{\mathrm{MC}}(t) + k_s C^i_{\mathrm{TS}}(t) S^i_{\mathrm{TS}}(t)]\,dt}, \tag{11b}$$

where $f_{h-\mathrm{MC}}$ is the fractional retention in MC during high flow, $f_{l-\mathrm{MC}}$ is the fractional retention in MC during

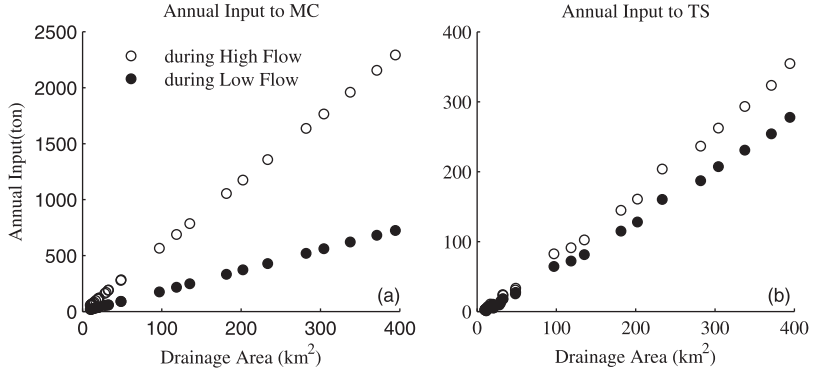

Figure 4. (a) Hillslope inputs into the MC zone as a function of drainage area, separately during high-flow and low-flow periods, respectively; and (b) exchange of nitrate from the MC zone into the TS zone, separately during high-flow and low-flow periods, respectively, as a function of watershed size.

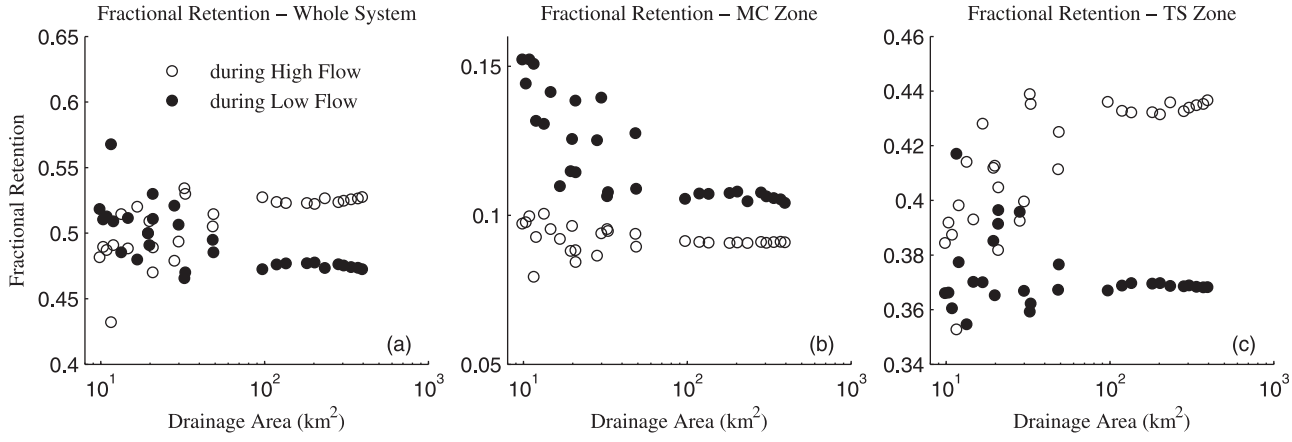

Figure 5. Fraction of retention separately during high-flow and low-flow periods, respectively, as a function of drainage area: (a) from the combined system (MC and TS zones together); (b) from the MC zone only; and (c) from the TS zone only.

low-flow period, T_h is the duration of high-flow period [T], T_l is the duration of low-flow period [T], and T is the total simulation period [T]. The results for fractions retained presented in Figure 5 indicate that even though the bulk loadings from hillslopes are vastly different during the two flow periods (e.g., 3.5 times larger during high flows, as shown in Figure 4), the magnitudes of the fractions retained are much closer in all three cases (certainly not 3.5 times different); the respective fractions (i.e., fractions of the total amounts of retention that occurred during the two periods) fall in the range 0.4–0.6. The retention fraction in the MC zone in the range 0.08–0.15 is much smaller than in the TS zone (in the range 0.35–0.45). We also find that in the case of the MC zone, the fraction retained during high-flow periods is low (0.1) and remains invariant with drainage area, whereas the fraction retained during low periods decreases with increasing drainage area. The situation is reversed in the TS zone: the fraction retained during high flows increases with increasing watershed area in the TS zone and remains invariant with drainage area during low-flow periods. These trends are similar to trends presented by *Wollheim et al.* [2008]. In all three cases, despite the sharp discrepancies in hillslope loading between high flows and low flows, the differences in the actual retention are much smaller.

[34] This compensation in fractional retention could be related to the retention efficiency: it may be higher during low flows, and lower during high flows. We will now look at the corresponding results for retention efficiency in more detail. The retention efficiency is defined as the ratio between the nitrate retained in MC or TS zone during high or low-flow period and the total nitrate load from the hillslope during the high or low-flow period. Figure 6 presents the estimated retention efficiencies at the watershed scale separately for the MC and TS zones, as well as for the combined system. The calculation of the retention efficiency in the MC zone is as follows:

$$Eff_{h-\mathrm{MC}} = \frac{\sum_i \int_{T_h} k_c C^i_{\mathrm{MC}}(t) S^i_{\mathrm{MC}}(t)\,dt}{\sum_i \int_{T_h} C^i_h(t) Q^i_h(t)\,dt}, \tag{12a}$$

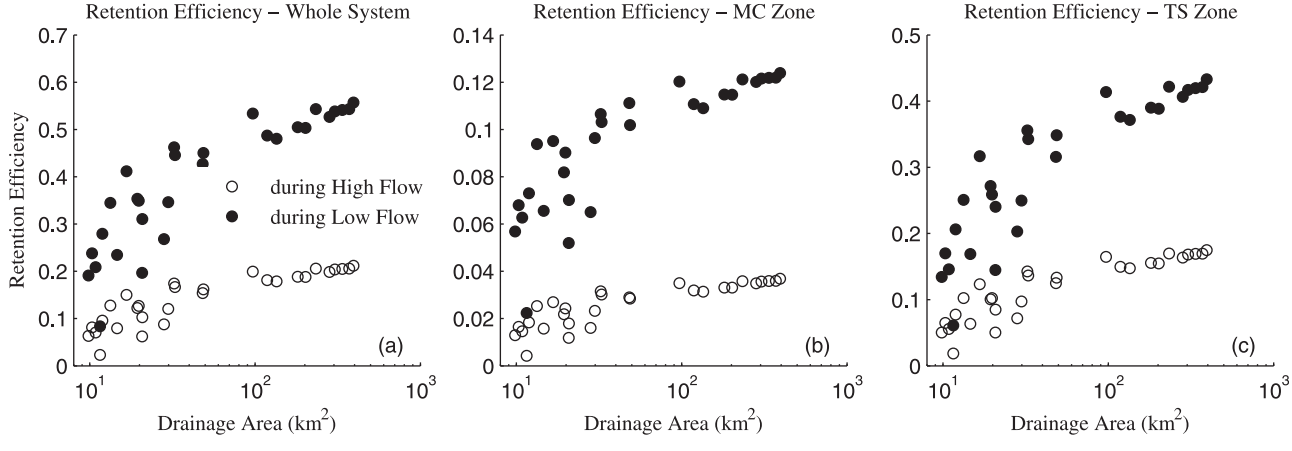

Figure 6. Retention efficiency estimated separately during high-flow and low-flow periods, respectively, as a function of drainage area: (a) from the combined system (MC and TS zones together); (b) from the MC zone only; and (c) from the TS zone only.

$$Eff_{l-\mathrm{MC}} = \frac{\sum_i \int_{T_l} k_c C^i_{\mathrm{MC}}(t) S^i_{\mathrm{MC}}(t) dt}{\sum_i \int_{T_l} C^i_h(t) Q^i_h(t) dt}, \quad (12b)$$

where $Eff_{h-\mathrm{MC}}$ is the retention efficiency within MC during high-flow periods, $Eff_{l-\mathrm{MC}}$ is the retention efficiency within MC during low-flow periods. The method for the calculation of retention efficiencies in the TS zone is similar. Figure 6 demonstrates that the retention efficiency during low flows is about three times higher than during high flows, in all three cases (whole system, as well as separately in the MC and TS zones), consistent with previous research that has noted that nitrate retention is most efficient during low-flow periods [*Alexander et al.*, 2009]. In all cases, the retention efficiency at the catchment scale is shown to increase with increasing drainage area. These results indicate that although the nitrate loading from hillslopes during high flows is over three times higher than during low flows (see Figure 4), the much smaller retention efficiencies during high flows (i.e., about a third of that during low flow) nearly compensates for the differences in hillslope loadings giving rise to somewhat equivalent values for fractional retention during high and low-flow periods, as shown in Figure 5 above.

[35] We further investigate the differences between the two sets of retention efficiencies, and if these can be explained by recourse to estimates of three different time scales: residence time in the main channel (τ_{MC}), nitrate reaction time in the MC zone (SRT-MC) and in the TS zone (SRT-TS). Following *Stewart et al.* [2011] and *Botter et al.* [2010], as a first attempt, we define these time scales for each REW as follows (using previous notation):

$$\tau_{\mathrm{MC}} = L/v, \quad (13a)$$

$$\text{SRT-MC} = h/v_c, \quad (13b)$$

$$\text{SRT-TS} = \frac{A_{\mathrm{MC}}/A_{\mathrm{TS}} + k_s/\alpha}{k_s}. \quad (13c)$$

[36] The corresponding time scales at the network scale are defined as follows:

$$T^i = \tau^i w^i + \sum T^j w^j, \quad (14a)$$

where

$$w^i = A^i/A^i_d \quad (14b)$$

and

$$w^j = A^j_d/A^i_d, \quad (14c)$$

where T^i is the total time within REW$_i$, T^j is the total time within all upstream REWs j, τ^i is the time within each reach (which can be either τ_{MC}, SRT-MC, or SRT-TS as per equations (13a), (13b), and (13c)), w^i is the weight for each component (which is related to the respective areas of the REWs), A^i is the area of REW$_i$, A^i_d is the drainage area of current REW$_i$, and A^j_d is the drainage area of the upstream reach j. We would expect the respective ratios of water residence time to solute reaction time (Damkohler number (*Da*) [*Ocampo et al.*, 2006]) to provide a first order indication of the efficiency of retention in both the MC and TS zones. Since the water exchange between MC and TS is assumed small enough to ignore in the paper, water residence time related to nutrient uptake in the TS zone is therefore assumed to be the same as in MC (τ).

[37] For the reason of brevity, we will not show detailed results of the network scale residence times or the reaction times (calculated from equation (14)) here. The trends in these numerical results are that the residence time during low flows is larger than during high flows for all watershed sizes, while the reaction times in the MC zone, SRT-MC, and in the TS zone, SRT-TS, show an opposite trend in that the reaction times are much larger during high flows than during low flows. This suggests larger ratios of residence times to reaction times (i.e., the Damkohler number *Da*), i.e., higher efficiencies during low-flow periods than during high-flow periods. The shorter reaction time in TS zone than in the MC zone leads to a larger Damkohler number in TS zone, i.e., higher (roughly 2 to 4 times) retention efficiency in the TS zone than in the MC zone (Figure 6). This explains the much larger fractional retention by TS than by MC zone shown in Figure 5 (about 4.5 times greater during high flow and 2.5 times during low flow).

3.2. Effects of Within-Year Hydrologic Variability on Retention Efficiency

[38] The results presented so far indicate significant differences between the loadings and retention efficiencies between high and low-flow periods, including the relative contributions of the MC and TS zones to the overall nitrate retention processes. One can therefore foresee that intra-annual streamflow variability, i.e., the strength of fluctuations of streamflows between high flows and low flows, can significantly impact net retention and overall retention efficiency at the watershed (space) scale and annual time scale. In order to assess the net effect of within-year hydrologic variability we constructed three different rainfall scenarios and implemented the coupled model under each of these scenarios in Monte Carlo fashion. Summary statistics for the rainfall inputs and for the resulting streamflows are presented in Table 1, where we quantified the intra-annual variability of flows in terms of the coefficient of variation, $CV(Q)$. The concentrations of nitrate inflows from hillslopes are still maintained at 15 NO_3-N mg L^{-1} throughout the year.

[39] Figure 7 presents the variation of retention efficiencies (nitrate retained during high/low-flow periods in MC/TS zone as percentage of total loading during those periods) as a function of watershed size for the three different climates considered (note that retention efficiency is the ratio of retention to net loading from the hillslopes). The results for the whole system (i.e., MC and TS zones together) indicate that the increase of hydrologic variability, as represented in the three climate scenarios, with climate 3 being most variable, leads to a reduction of retention efficiencies in the combined system, during high-flow periods.

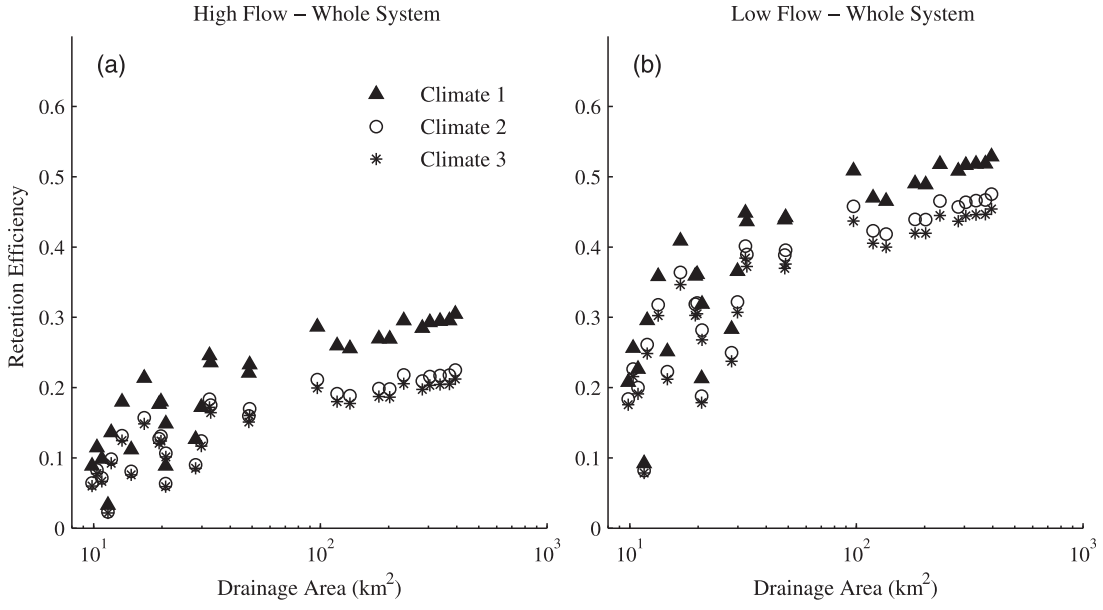

Figure 7. Watershed scale retention efficiencies as a function of drainage area for climate 1 (p = 0.4 mm h^{-1}, t_r = 34 h, t_b = 76 h), climate 2 (p = 0.8 mm h^{-1}, t_r = 34 h, t_b = 186 h), and climate 3 (p = 2.0 mm h^{-1}, t_r = 15 h, t_b = 227 h) for the whole system (MC and TS): (a) high-flow periods and (b) low-flow periods.

3.3. Scale Effects: Relative Roles of Biogeochemical and Geomorphologic Factors

[40] So far we have explored the partitioning of retention fractions between high-flow and low-flow periods, and the breakdown of the contributions of the MC and TS zones to total retention. The analyses have revealed that ultimately these can be explained in terms of retention efficiencies and a competition between residence times and reaction times. Along the way we also discovered that the richness of distribution of bulk uptakes and retention efficiencies also systematically change with increasing watershed size.

[41] The default parameterizations that we have adopted in the simulations so far have assumed that the thickness of the TS zone is constant across the entire network. In view of the demonstrated importance of the TS zone, what impact does this assumption have on the scaling behavior of nutrient retention? Similarly, we have assumed that the uptake rate in the MC zone is equal to $k_c = v_c/h$. By making this assumption, we are ensuring that the nutrient retention in the MC zone becomes less efficient as we move from headwater streams to the much deeper, higher order streams. Although the plankton in the water column also contributes to the nutrient retention, given the relatively shallower water column and shorter residence time available for uptake, it is relatively minor compared to the benthic uptake. Therefore in this paper we will focus on the impact of the TS depth. These are important questions because there is as of yet very little empirical evidence for these rather strong assumptions: whether the thickness of the TS zone remains constant downstream or increases with the increase in the spatial scale. In order to generate insights into their relative effects on the predicted scaling behavior, we carried out a new set of simulations where we allowed the thickness of the TS zone to increase in the downstream direction, in such a way as to maintain a constant A_{TS}/A_{MC} ratio at a value of 0.35 [*Briggs et al.*, 2010].

[42] Figure 8 presents a comparison of two events (approximately 25 days) in the 10-year long time series of retention rates from the MC and TS zones, corresponding to climate 2, and for two different scenarios: (a) thickness of TS remains constant across the network and (b) thickness of TS increases in downstream direction (A_{TS}/A_{MC} is held constant at 0.35), while in both scenarios v_c is held constant at 0.002 m h^{-1}. This part of the model sensitivity analyses with respect to the size of the TS zone is summarized in the top half of Table 3. The results are presented for a headwater stream and for the stream at the watershed outlet. The results indicate that, for varying k_c ($k_c = v_c/h$, v_c = constant), increase of A_{TS} in the downstream direction leads to much higher retention from the TS zone with increasing watershed size: the retention rate at the outlet stream increases from around 7 to 12 kg h^{-1} when A_{TS} becomes larger in the downstream direction (Figures 8b and 8d), while the retention rate in MC does not change.

[43] Figure 9 summarizes the results of this sensitivity analyses (i.e., with respect to the size of the TS zone, as summarized in the top half of Table 3) in terms of (1) the fraction contributed to total retention (over the whole year) by the MC zone, and (2) the fractional retention from the combined (MC and TS) system during high-flow periods. The results in Figure 9a indicate that the fractional retention contributed by the MC zone is much less when the size of the TS zone is allowed to increase in the downstream direction. Figure 9b presents the corresponding results for the fractional retention during high flows for the combined system. When k_c decreases downstream, the assumption of variable TS size makes a bigger contribution to the fraction retained during high flows.

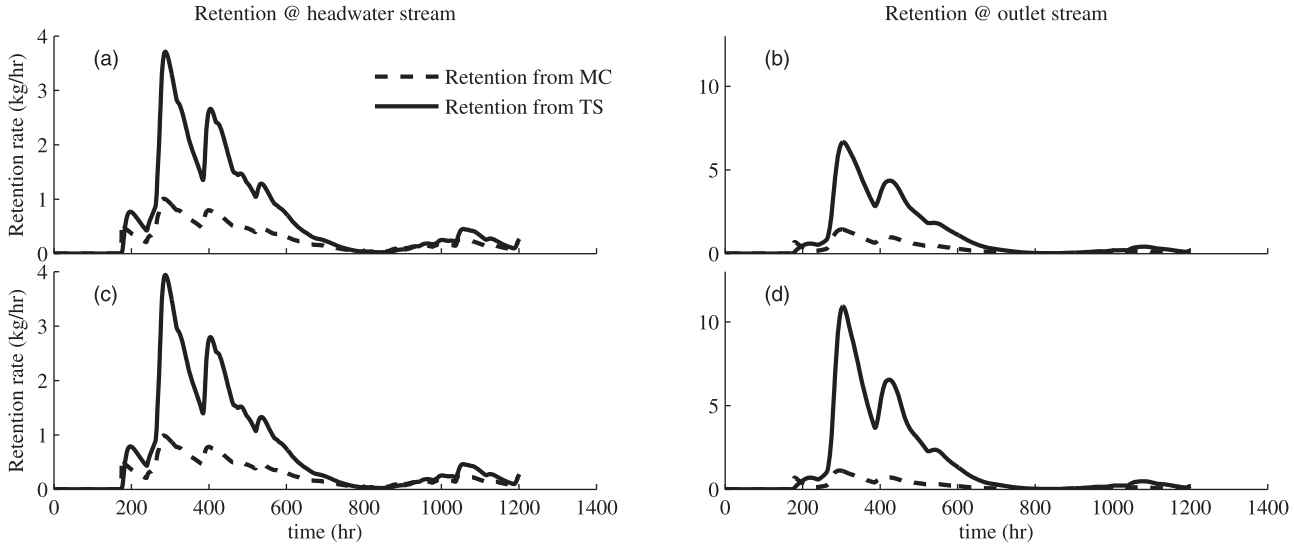

Figure 8. Schematic describing retention rates (from MC and TS zones) for two parameter combinations: case 1 (a) and (b): v_c maintained constant at 0.002 m h^{-1}, thickness of the TS zone maintained constant; case 2 (c) and (d): v_c maintained constant at 0.002 m h^{-1}, thickness of the TS zone increases in the downstream direction, with the ratio A_{TS}/A_{MC} maintained constant at 0.35: (a) and (c) retention rates for a headwater stream; (b) and (d) retention rates for the higher order stream at the outlet.

4. Discussion of Results

[44] The results presented have demonstrated that there are substantial differences between nutrient retention rates during high-flow and low-flow periods. The differences are due to (1) variability in hillslope water and nitrate inputs, leading to differences in flow depth, velocity, and nutrient concentration, and (2) the differing roles and contributions from the MC and TS zones, leading to differences in retention efficiencies. Similar differences are observed between the contribution from MC and TS, which can be related to the parameters chosen in the simulations and the assumptions about the scaling affect arising from the parameters chosen (v_c and k_s). In the following we seek generalizable insights based on the use of the model, and manipulation of model predictions: reaction times (governed by both the solute transport properties, flow depth, and the relative sizes of the MC and TS zones, which are indirectly affected by variable flow depths).

4.1. Effects of Hydrologic Variability: Bulk Parameterization Based on Time Scales

[45] In Figure 7 we demonstrated that within-year hydrologic variability can have a significant impact on net retention at the watershed scale, especially during high-flow periods. In particular, increasing variability leads to decreasing retention efficiency. This can be attributed to faster velocities and hence shorter residence times, provided the reaction times remain relatively invariant.

[46] The effect of hydrologic variability and the connection to residence times is illustrated in Figure 10. In this figure we first express the strength of retention for all three climate scenarios in terms of a watershed scale delivery ratio *DR* (1-retention efficiency), the percentage of nutrient exported. The delivery ratio *DR* estimated for the three climates is then presented as a function of residence time in the river network τ_{MC} (in a semilog plot), for the whole year as well as for the high-flow and low-flow periods. The

Table 3. Summary of Different Scenarios Simulated in Sensitivity Analyses Involving Combinations of Climate, Geomorphology, and Biogeochemistry

		Climate 1	Climate 2	Climate 3
Impact of TS depth	TS depth constant	Low streamflow variability, TS depth constant with TS dominance	Intermediate streamflow variability, TS depth constant with TS dominance (base experiment)	High streamflow variability, TS depth constant with TS dominance
	TS depth increases downstream	Low streamflow variability, TS depth constant with TS dominance	Intermediate streamflow variability, TS depth constant with TS dominance	High streamflow variability, TS depth constant with TS dominance
Impact of v_c, k_s	TS dominant ($v_c = 0.002$ m h^{-1}, $k_s = 0.2$/h)		Intermediate streamflow variability, TS depth constant with TS dominance (base experiment)	
	MC, TS eq ($v_c = 0.002$ m h^{-1}, $k_s = 0.05$/h)		Intermediate streamflow variability, TS depth constant with eq MC, TS dominance	
	MC dominant ($v_c = 0.02$ m h^{-1}, $k_s = 0.2$/h)		Intermediate streamflow variability, TS depth constant with MC dominance	

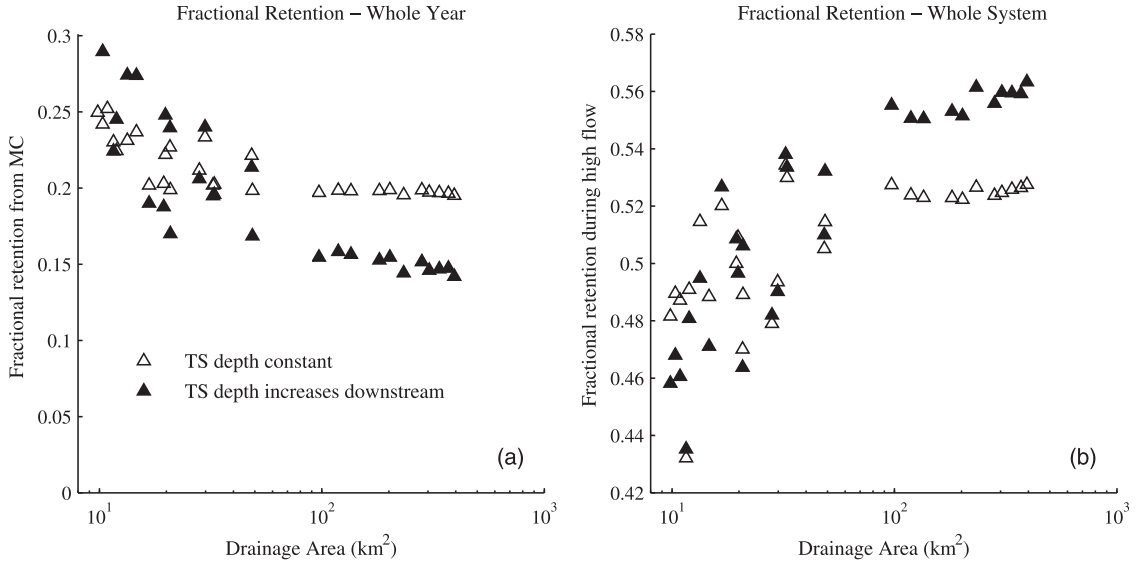

Figure 9. (a) Fractional retention from the MC zone over the whole year, and (b) fractional retention during high flows over the combined system (MC and TS zones together), both as functions of drainage area. These results are presented two scenarios of A_{TS}/A_{MC} ratio: (1) A_{TS} constant, and (2) A_{TS} increases downstream ($A_{TS}/A_{MC} = 0.35$).

results indicate that (1) there is an almost exponential relationship between *DR* and τ_{MC} (as reflected in the straight lines in the semilog plots), and (2) the slopes of the lines tend to decrease with increasing hydrologic variability, for all flow periods (Figure 10). This confirms that the first order control of *DR* (and hence the retention efficiency) is the residence time distribution. We then fitted the empirical *DR* versus τ_{MC} relationship to the following function: $DR = \exp(-k_e\tau_{MC})$, and estimated k_e, which can be deemed as a first-order rate coefficient k_e at the watershed scale, and can be seen as a net measure of nutrient retention. Estimated values of k_e for the three climates, during high and low-flow periods, are presented in Table 1 and indicate that estimated k_e values decrease with increasing streamflow variability, and increases with the increment in TS zone size.

4.2. Scaling Effect: Relative Roles of Nutrient Uptake and Geomorphologic Factors

[47] The results presented so far have demonstrated the importance of the ratio between water residence time and solute reaction time. Two factors that play important roles in governing the estimates of both residence and reaction times are the flow condition in the stream, and the relative magnitudes of the nutrient uptake parameters k_c and k_s, and how they change in time and space (across the river

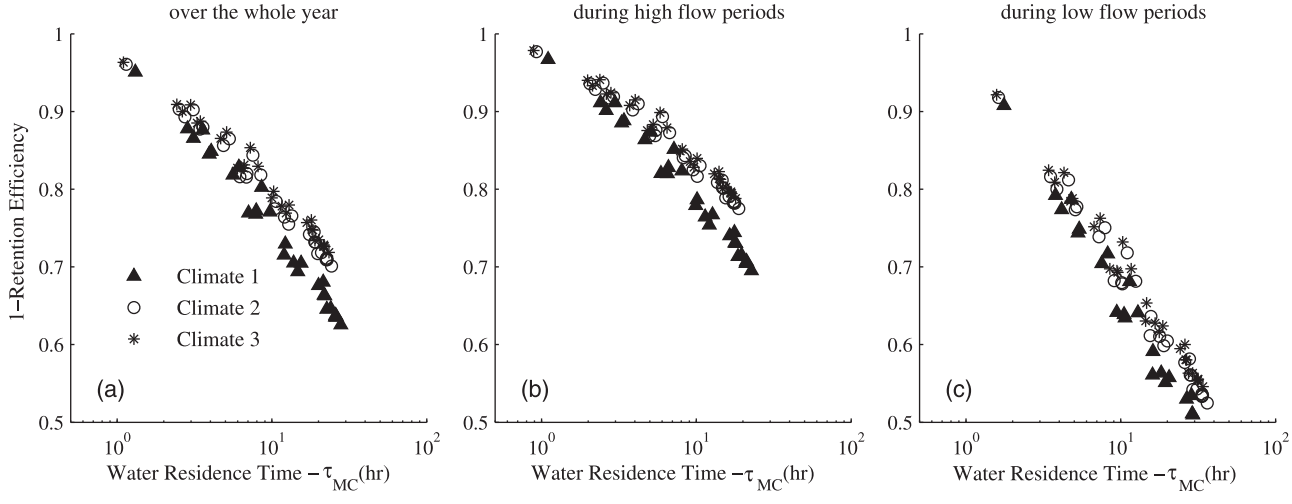

Figure 10. Catchment scale delivery ratio 1-retention efficiency as a function of weighted residence time τ_{MC} (as a surrogate for drainage area) for climate 1 ($p = 0.4$ mm h^{-1}, $t_r = 34$ h, $t_b = 76$ h), climate 2 ($p = 0.8$ mm h^{-1}, $t_r = 34$ h, $t_b = 186$ h), and climate 3 ($p = 2.0$ mm h^{-1}, $t_r = 15$ h, $t_b = 227$ h: (a) for the whole year; (b) during high-flow periods; and (c) during low-flow periods.

network). Flow state determines (a) velocity v, which governs residence time τ_{MC}, (b) flow depth h, which in combination with k_c governs reaction time in the MC zone, SRT-MC, and (c) the ratio A_{TS}/A_{MC}, with both A_{MC} and A_{TS} changing with the magnitude of flow, which together with k_c and k_s determines reaction time in the TS zone, SRT-TS.

[48] Because of the paucity of consistent empirical data across diverse field experiments, we made several assumptions in the parameterizations chosen for the base experiment: (1) that the TS retention is more dominant than MC, through adoption of $v_c = 0.002$ m h^{-1} and $k_s = 0.2$/h; (2) that the benthic uptake and retention is dominant over pelagic uptake, by setting the retention rate in the MC to decrease with flow depth ($k_c = v_c/h$); (3) that the TS depth is constant from headwater to outlet, by setting the TS depth to be constant at 0.06 m. These assumptions are critical to understanding and interpreting the model results presented in Figures 8 and 9, and summarized in terms of the effective rate coefficient k_e in Table 1 since they are likely to impact the results of the base experiment and the effects of the three climate scenarios chosen.

[49] In order to generate insights into these effects, we carried out sensitivity analyses with the model under a new set of scenarios, where (1) TS is the major contributor; (2) the contributions from TS and MC are roughly equivalent, and (3) the retention from MC is more dominant. The combinations of parameter values chosen for each of these scenarios are presented in the bottom half of Table 3. Figure 11 presents the impacts of various combinations of v_c and k_s in terms of (1) the fraction contributed to total retention (over the whole year) by the MC zone and (2) the fractional retention from the combined (MC and TS) system during high-flow periods. The results in Figure 11a indicate that with a smaller k_s or a larger v_c, the fractional retention from MC will increase equally across the entire network. Figure 11b presents the corresponding results for the fractional retention during high flows for the combined system. The combination with largest v_c and k_s values contributes to higher uptake and removal during high-flow periods.

[50] The sensitivity analysis with respect to the combination of v_c and k_s values (Figure 11) demonstrates that although the magnitudes of contributions from MC and TS change with the different parameter combinations adopted, and the contribution of TS decreases with the retention rate in TS (k_s), the resulting change is uniform from headwater streams to the outlet. That is, the scaling effect of the MC and TS contributions remains, and so does the impact of hydrologic variability on the retention efficiencies during high-flow and low-flow periods in the MC and TS zones (details not presented here for brevity).

[51] The sensitivity analysis with respect to the TS thickness indicates that the scaling effect of the contribution of MC can be amplified or attenuated by the TS zone thickness. For streams where benthic uptake is dominant, increasing TS zone thickness in the downstream direction adds further to the decrease in the fractional retention from the MC zone from headwater streams to the watershed outlet. These results suggest that, when considering nutrient retention at the watershed scale, especially when they include large rivers, the scaling of TS thickness in the downstream direction can be more important than the actual retention rate. Further experiments and modeling need to be done to parameterize the effects of both the morphology and the biogeochemistry of the transient storage zone.

5. Conclusions

[52] One of the main conclusions from this numerical modeling study is that, within the limitations of the model (for example, the assumption of first order kinetics), retention of dissolved nutrients during high-flow periods can

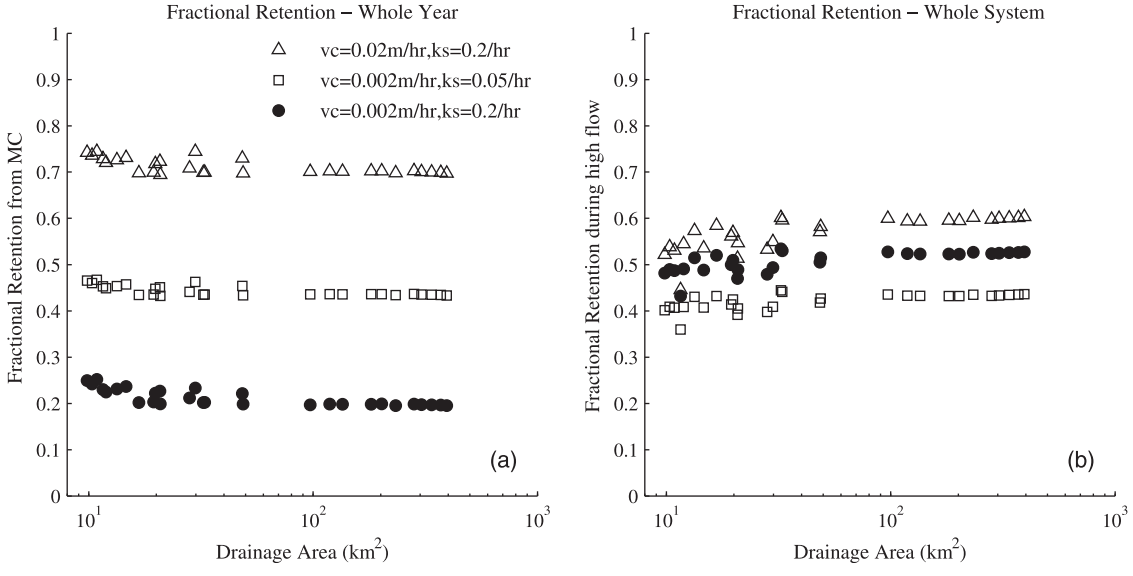

Figure 11. The three combinations of v_c and k_s impact on (a) fractional retention from the MC zone over the whole year, and (b) fractional retention during high flows over the combined system (MC and TS zones together), both as functions of drainage area. These results are presented for three different combinations of k_s and v_c: (1) MC dominant, $v_c = 0.02$ m h^{-1} and $k_s = 0.2$ h^{-1}, (2) MC and TS are equivalent, $v_c = 0.002$ m h^{-1} and $k_s = 0.05$/h, and (3) TS dominant, $v_c = 0.002$ m h^{-1} and $k_s = 0.2$/h.

indeed be significant, and should not be ignored. For the parameter combinations used in this study, the total mass retained during high flows constitutes ~50% of the total annual retention. This is in spite of the much lower retention efficiencies during high flows compared to during low-flow periods. This can be attributed to much larger loading during high flows, which overwhelms the reduced retention efficiency, and leads to an overall higher retention of total N mass in the system. This difference in nutrient load is quite significant in the MC zone but is much smaller in the TS zone since the residence time helps modulate the concentration gradients to limit the nutrient access to TS zone. While previous studies have focused primarily on the decrease in the nutrient retention efficiency during storm events, we showed for the first time that despite the reduced efficiency total mass retention is greater than during base flow. This result is similar to the findings of *Ensign et al.* [2006] who noted strong ammonium retention during storm events in a coastal agricultural stream in North Carolina. This observation calls for increased focus on understanding nutrient dynamics during storm events.

[53] Moreover, an important consequence of the retention during high-flow periods is that the nature of within-year variability of streamflows can have a significant impact on the bulk retention, delivery ratio, and retention efficiency. This is due to the differences between the rates of retention and the dominant retention mechanisms as streamflows change over the range from low to high flows. Our model simulations demonstrated that intra-annual streamflow variability does have a significant impact on retention rates at all scales: the more variable the streamflow is, compared to mean discharge, the less nitrate is retained in the channel network (i.e., greater export). A first order uptake rate estimated at the scale of the whole third order network k_e was seen to decrease with increased streamflow variability. While the importance of intra-annual variability has already been highlighted in previous studies [i.e., *Wollheim et al.* 2008; *Botter et al.* 2010], and in particular the companion paper by *Basu et al.* [2011], the results presented in this paper for the first time quantify this effect by systematically simulating precipitation events of different frequencies and intensities. Climate change is forecast to alter the rainfall frequencies and intensities more severely than the mean values, contributing to increased within-year variability, which can translate to a reduction in nutrient removal efficiencies, thus exacerbating critical concerns about increased N export. Consequently, further investigations into the effect of the intra-annual rainfall variability on nutrient retention are critical.

[54] Finally, the contributions of high-flow periods to total annual bulk retention is further enhanced in large rivers, even as the efficiency of retention decreases from headwater to higher order streams, and to large rivers. This too can be explained through recourse to the increase of loading in larger rivers compared to headwater streams. We have demonstrated in this study for the first time that despite reduced efficiency in nutrient retention with river size, the total mass retention is greater in larger rivers thus necessitating increased focus on understanding nutrient dynamics in larger rivers. Further experiments focusing on nutrient spiraling in larger rivers are therefore critically needed [e.g., *Tank et al.*, 2008].

[55] Clearly there is considerable room for the model we presented here to be substantially improved. A recent review paper has highlighted key areas in which the current generation of nitrate cycling models at the river network scale needs to be advanced [*Helton et al.*, 2011]. There is currently insufficient information and understanding to adequately constrain parameterizations (i.e., functional forms) of the various processes. For example, not much is known about the relative contributions of benthic and pelagic uptake, or the partitioning of retention between the TS and MC zones, their dependence on flow and environmental conditions (e.g., temperature, turbidity, nutrient concentrations, see *Covino et al.* [2010b]), and how these processes scale across stream networks and flow states. Similarly, the conceptual approach we have adopted to simulate the effects of the TS zone is highly restrictive, and poses problems toward its parameterization. These call for further detailed field investigations in large rivers, during both low- and high-flow events.

[56] We recognize that modeling gross retention of dissolved nitrogen in a stream network is simplistic, and processes like mineralization, groundwater inputs, or the role of particulate nitrogen could also be important. A pseudo-steady state (inputs = outputs) during base flow has been observed in four southeastern small streams [*Brookshire et al.*, 2009], where uptake was compensated by remineralization and groundwater inputs. However, because of lack of adequate information (i.e., mineralization rates of N, concentration of groundwater recharge, or concentrations of PON); here we have focused primarily on gross nitrogen retention. Gross nutrient retention has commonly been measured during base flow periods in small streams, and very few studies have explored the effect of within-year streamflow variations on this metric as a function of spatial scale of observation. However, the model we presented here can be extended to study the questions on particulate versus dissolved, organic versus inorganic nitrogen, and gross nitrogen retention versus mineralization in stream ecosystems in future studies. Given the importance of the impact of nutrient concentration on uptake, more field measurements quantifying the relationship between nutrient concentration and uptake within a single stream system at different catchment scales [e.g., *Earl et al.*, 2006; *Covino et al.*, 2010a; *Covino et al.*, 2010b] will be crucial for improving the ability of numerical models to simulate nutrient uptake over a range of nutrient concentrations. Finally, here we have chosen a simple bucket model to represent the hillslope contributions, where we arbitrarily assumed a constant concentration of hillslope inputs, which is clearly not realistic. A more sophisticated hillslope model with both hydrologic and biogeochemical components is needed, and is crucial to investigating the effects of land use changes on nutrient export. Clearly, these extensions are beyond the scope of the present modeling study, and are left for future research.

[57] **Acknowledgments.** Work on this paper commenced during the Summer Institute organized at the University of British Columbia (UBC) during June–July 2009 as part of the NSF-funded project: *Water Cycle Dynamics in a Changing Environment: Advancing Hydrologic Science through Synthesis* (NSF grant EAR-0636043, M. Sivapalan, PI). Thanks also due to Marwan Hassan and the Department of Geography of UBC for hosting the Summer Institute and for providing outstanding facilities. Work on the paper was also partially supported by NSF-Project: *Using Empirical and Modeling Approaches to Quantify the Importance of Nutrient Spiraling in Rivers* (grant DEB-0922118, Jennifer Tank, PI).

References

Alexander, R. B., J. K. Böhlke, E. W. Boyer, M. B. David, J. W. Harvey, P. J. Mulholland, S. P. Seitzinger, C. R. Tobias, C. Tonitto, and W. M. Wollheim (2009), Dynamic modeling of nitrogen losses in river networks unravels the coupled effects of hydrological and biogeochemical processes, *Biogeochemistry*, *93*, 91–116.

Algoazany, A. S. (2006), Long-term effects of agricultural chemicals and management practices on water quality in a subsurface drained watershed, PhD thesis, 258 pp., Univ. of Ill. at Urbana-Champaign, Urbana.

Basu, N. B., P. S. C. Rao, H. Winzeler, S. Kumar, P. Owens, and V. Merwade (2009), Parsimonious modeling of hydrologic responses in engineered watersheds: Structural heterogeneity versus functional homogeneity, *Water Resour. Res.*, *46*, W04501, doi:10.1029/2009WR007803.

Basu, N. B., P. S. C. Rao, S. E. Thompson, N. V. Loukinova, S. D. Donner, S. Ye, and M. Sivapalan (2011), Spatiotemporal averaging of in-stream solute removal dynamics, *Water Resour. Res.*, *47*, W00J06, doi:10.1029/2010WR010196.

Bencala, K. E., and R. A. Walters (1983), Simulation of solute transport in a mountain pool and riffle stream: A transient storage model, *Water Resour. Res.*, *19*(3), 718–724.

Böhlke, J. K., R. C. Antweiler, J. W. Harvey, A. E. Laursen, L. K. Smith, R. L. Smith, and M. A. Voytek (2009), Multi-scale measurements and modeling of denitrification in streams with varying flow and nitrate concentration in the upper Mississippi River basin, USA, *Biogeochemistry*, *93*, 117–141.

Botter, G., N. B. Basu, S. Zanardo, P. S. C. Rao, and A. Rinaldo (2010), Stochastic modeling of nutrient losses in streams: Interactions of climatic, hydrologic, and biogeochemical controls, *Water Resour. Res.*, *46*, W08509, doi:10.1029/2009WR008758.

Briggs, M. A., M. N. Gooseff, B. J. Peterson, K. Morkeski, W. M. Wollheim, and C. S. Hopkinson (2010), Surface and hyporheic transient storage dynamics throughout a coastal stream network, *Water Resour. Res.*, *46*, W06516, doi:10.1029/2009WR008222.

Brookshire, E. N. J., H. M. Valett, and S. Gerber (2009), Maintenance of terrestrial nutrient loss signatures during in-stream transport, *Ecology*, *90*, 293–299.

Claessens, L., and C. L. Tague (2009), Transport-based method for estimating in-stream nitrogen uptake at ambient concentration from nutrient addition experiments, *Limnol. Oceanogr. Methods*, *7*, 811–822.

Claessens, L., C. L. Tague, P. M. Groffman, and J. M. Melack (2009), Longitudinal assessment of the effect of concentration on stream N uptake rates in an urbanizing watershed, *Biogeochemistry*, *98*, 67–74, doi:10.1007/s10533-009-9376-y.

Covino, T. P., B. L. McGlynn, and R. A. McNamara (2010a), Tracer additions for spiraling curve characterization (TASCC): Quantifying stream nutrient uptake kinetics from ambient to saturation, *Limnol. Oceanogr. Methods*, *8*, 484–498.

Covino, T. P., B. L. McGlynn, and M. A. Baker (2010b), Separating physical and biological nutrient retention and quantifying uptake kinetics from ambient to saturation in successive mountain stream reaches, *J. Geophys. Res. Biogeosci.*, *115*, G04010.

De Smedt, F., W. Brevis, and P. Debels (2005), Analytical solution for solute transport resulting from instantaneous injection in streams with transient storage, *J. Hydrol.*, *315*, 25–39.

Dodds, W. K., et al. (2002), N uptake as a function of concentration in streams, *J. North Am. Benthol. Soc.*, *21*(2), 206–220.

Donner, S. D., M. T. Coe, J. D. Lenters, T. E. Twine, and J. A. Foley (2002), Modeling the impact of hydrological changes on nitrate transport in the Mississippi river basin from 1955 to 1994, *Global Biogeochem. Cycles*, *16*(3), 1043, 10.1029/2001GB001396.

Dunn, D. D. (1996), Trends in nutrient inflows to the Gulf of Mexico from streams draining the conterminous United States 1972–1993. *US Geol. Surv., Water-Res. Invest. Rep.*, 96-4113, US Geol. Surv., Austin, TX, 60 pp.

Earl, S. R., H. M. Valett, and J. R. Webster (2006), Nitrogen saturation in stream ecosystems, *Ecology*, *87*(12), 3140–3151.

Ensign, S. H., and M. W. Doyle (2006), Nutrient spiraling in streams and river networks, *J. Geophys. Res.*, *111*, G04009, doi:10.1029/2005JG000114.

Ensign, S. H., S. K. McMillan, S. P. Thompson, and M. F. Piehler (2006), Nitrogen and phosphorus attenuation within the stream network of a coastal, agricultural watershed, *J. Environ. Qual.*, *35*, 1237–1247.

Goolsby, D. A., W. A. Battaglin, B. T. Aulenbach, and R. P. Hooper (2000), Nitrogen flux and sources in the Mississippi River Basin, *Sci. Total Environ.*, *248*, 75–86.

Guan, K., S. E. Thompson, C. J. Harman, N. B. Basu, P. S. C. Rao, M. Sivapalan, A. I. Packman, and P. K. Kalita (2011), Spatiotemporal scaling of hydrological and agrochemical export dynamics in a tile-drained Midwestern watershed, *Water Resour. Res.*, *47*, W00J02, doi:10.1029/2010WR009997.

Hall, R. O., Jr., and J. Tank (2003), Ecosystem metabolism controls nitrogen uptake in streams in Grand Teton National Park, Wyoming, *Limnol. Oceanogr.*, *48*(3), 1120–1128.

Hall, R. O., B. J. Peterson, and J. L. Meyer (1998), Testing a nitrogen cycling model of a forest stream by using a nitrogen-15 tracer addition, *Ecosystems*, *1*, 283–298.

Hall, R. O., Jr., E. S. Bernhardt, and G. E. Likens (2002), Relating nutrient uptake with transient storage in forested mountain streams, *Limnol. Oceanogr.*, *47*(1), 255–265.

Hall, R. O., Jr., et al. (2009a), Nitrate removal in stream ecosystems measured by ^{15}N addition experiments: Total uptake, *Limnol. Oceanogr.*, *54*(3), 653–665.

Hall, R. O., Jr., M. A. Baker, C. D. Arp, and B. J. Koch (2009b), Hydrologic control of nitrogen removal, storage, and export in a mountain stream, *Limnol. Oceanogr.*, *54*(6), 2128–2142.

Harman, C. J., P. S. C. Rao, N. B. Basu, G. S. McGrath, P. Kumar, and M. Sivapalan (2011), Climate, soil and vegetation controls on the temporal variability of vadose zone transport, *Water Resour. Res.*, *47*, W00J13, doi:10.1029/2010WR010194.

Helton, A. M., et al. (2011), Thinking outside the channel: Modeling nitrogen cycling in networked river ecosystems, *Front. Ecol. Environ.*, *9*(4), 229–238, doi:10.1890/080211.

Li, H., and M. Sivapalan (2011), Effect of spatial heterogeneity of runoff generation mechanisms on the scaling behavior of event runoff responses in a natural river basin, *Water Resour. Res.*, *47*, W00H08, doi:10.1029/2010WR009712.

Li, H., M. Sivapalan, D. Liu, and F. Tian (2010), Water and nutrient balances in a large tile-drained agricultural catchment: A distributed modeling study, *Hydrol. Earth Syst. Sci.*, *14*, 2259–2275, doi:10.5194/hess-14-2259-2010.

Lyne, V., and M. H. Hollick (1979), Stochastic time-variable rainfall-runoff modelling, *Proc. Hydrology and Water Resources Symposium, Perth*, pp. 89–92, Institute of Engineers, Australia.

Marti, E., N. B. Grimm, and S. G. Fisher (1997), Pre- and postflood retention efficiency of nitrogen in a Sonoran Desert stream, *J. North Am. Benthol. Soc.*, *16*, 805–819.

Mitchell, J. K., G. F. McIsaac, S. E. Walker, and M. C. Hirschi (2000), Nitrate in river and subsurface drainage flows from an east central Illinois watershed, *Trans. ASAE*, *43*(2), 337–342.

Mulholland, P. J., and D. L. DeAngelis (2000), Effect of surface/subsurface exchange on nutrient dynamics and nutrient spiraling in streams, in *Streams and Ground Waters*, edited by J. B. Jones, Jr. and P. J. Mulholland, pp. 149–166, Academic, San Diego, CA.

Mulholland, P. J., et al. (2002), Can uptake length in stream be determined by nutrient addition experiments? Results from an inter-biome comparison study, *J. North Am. Benthol. Soc.*, *21*(4), 504–560.

Mulholland, P. J., et al. (2008), Stream denitrification across biomes and its response to anthropogenic nitrate loading. *Nature*, *452*, 202–205.

Newbold, J. D., P. J. Mulholland, J. W. Elwood, and R. V. O'Neill (1982), Organic-carbon spiraling in stream ecosystems, *Oikos*, *38*, 266–272.

O'Brien, J. M., W. K. Dodds, K. C. Wilson, J. N. Murdock, and J. Eichmiller (2007), The saturation of N cycling in Central Plains streams: 15N experiments across abroad gradient of nitrate concentrations, *Biogeochemistry*, *84*, 31–49, doi:10.1007/s10533-007-9073-7.

Ocampo, C. J., C. E. Oldham, and M. Sivapalan (2006), Nitrate attenuation in agricultural catchments: Shifting balances between transport and reaction, *Water Resour. Res.*, *42*, W01408, doi:10.1029/2004WR003773.

Paul, M. J., and R. O. Hall (2002), Particle transport and transient storage along a stream size gradient in the Hubbard Brook Experimental Forest, *J. North Am. Benthol. Soc.*, *21*(2), 195–205.

Payn, R. A., M. N. Gooseff, D. A. Benson, O. A. Cirpka, J. A. Zarnetske, W. B. Bowden, J. P. McNamara, and J. H. Bradford (2008), Comparison of instantaneous and constant-rate tracer experiments through non-parametric analysis of residence time distributions, *Water Resour. Res.*, *44*, W06404, doi:10.1029/2007WR006274.

Peterson, B. J., et al. (2001), Control of nitrogen export from watersheds by headwater streams, *Science*, *292*(5514), 86–90.

Rabalais, N. N., R. E. Turner, and W. J. Wiseman, Jr. (2002), Gulf of Mexico hypoxia, aka "the dead zone," *Annu. Rev. Ecol. Syst.*, *33*, 235–263.

Reggiani, P., M. Sivapalan, and S. M. Hassanizadeh (1998), A unifying framework for catchment thermodynamics: Balance equations for mass,

momentum, energy and entropy, and the second law of thermodynamics, *Adv. Water Resour.*, *22*, 367–398.

Reggiani, P., S. M. Hassanizadeh, and M. Sivapalan (1999), A unifying framework for watershed thermodynamics: Constitutive relationships, *Adv. Water Resour.*, *23*, 15–39.

Reggiani, P., M. Sivapalan, S. M. Hassanizadeh, and W. G. Gray (2001), Coupled equations for mass and momentum balance in a bifurcating stream channel network: Theoretical derivation and computational experiments, *Proc. R. Soc. Ser. A. Math. Phys. Eng. Sci.*, *457*, 157–189.

Robinson, J. S., and M. Sivapalan (1997), Temporal scales and hydrological regimes: Implications for flood frequency scaling, *Water Resour. Res.*, *33*(12), 2981–2999.

Robinson, J. S., M. Sivapalan, and J. D. Snell (1995), On the relative roles of hillslope processes, channel routing and network geomorphology in the hydrological response of natural catchments, *Water Resour. Res.*, *31*(12), 3089–3101.

Royer, T. V., M. B. David, and L. E. Gentry (2006), Timing of riverine export of nitrate and phosphorus from agricultural watersheds in Illinois: Implications for reducing nutrient loading to the Mississippi River, *Environ. Sci. Technol.*, *40*, 4126–4131.

Runkel, R. L. (1998), One dimensional transport with inflow and storage (OTIS): A solute transport model for streams and rivers, *U.S. Geol. Surv. Water Resour. Invest. Rep.*, *98-4018*, 73 pp.

Runkel, R. L. (2000), Using OTIS to model solute transport in streams and rivers, *U.S. Geol. Surv. Fact Sheet*, *FS-138-99*, 4 pp.

Runkel, R. L. (2007), Toward a transport-based analysis of nutrient spiraling and uptake in streams, *Limnol. Oceanogr. Methods*, *5*, 50–62.

Runkel, R. L., and K. E. Bencala (1995), Transport of reacting solutes in rivers and streams, in *Environmental Hydrology*, edited by V. P. Singh, pp. 137–164, Kluwer Academic, Dordrecht, The Netherlands.

Seitzinger, S. P., R. V. Styles, E. W. Boyer, R. B. Alexander, G. Billen, R. W. Howarth, B. Mayer, and N. V. Breemen (2002), Nitrogen retention in rivers: Model development and application to watersheds in the northeastern U.S.A., *Biogeochemistry*, *57/58*, 199–237.

Smith, R. A., G. E. Schwarz, and R. B. Alexander (1997), Regional interpretation of water quality monitoring data, *Water Resour. Res.*, *33*(12), 2781–2798.

Stall, J. B., and Y. S. Fok (1968), Hydraulic geometry of Illinois streams, *Illinois State Water Survey Rep., CR-92*, 47 pp., Univ. of Ill. at Urbana-Champaign, Urbana.

Stewart, R. J., W. M. Wollheim, M. N. Gooseff, M. A. Briggs, J. M. Jacobs, B. J. Peterson, and C. S. Hopkinson (2011), Separation of river network-scale nitrogen removal among main channel and two transient storage compartments, *Water Resour. Res.*, *47*, W00J10, doi:10.1029/2010WR009896.

Stofleth, J. M., F. D. Shields Jr., and G. A. Fox (2008), Hyporheic and total transient storage in small, sand-bed streams, *Hydrol. Processes*, *22*, 1885–1894.

Stream Solute Workshop (1990), Concepts and methods for assessing solute dynamics in stream ecosystems, *J. North Am. Benthol. Soc.*, *9*(2), 95–119.

Tank, J. L., E. J. Rosi-Marshall, M. A. Baker, and R. O. Hall, Jr. (2008), Are rivers just big streams? A pulse method to quantify nitrogen demand in a large river, *Ecology*, *89*(10), 2935–2945.

Thompson, S. E., N. B. Basu, J. Lascurain Jr., A. Aubeneau, and P. S. C. Rao (2011), Relative dominance of hydrologic versus biogeochemical factors on solute export across impact gradients, *Water Resour. Res.*, *47*, W00J05, doi:10.1029/2010WR009605.

Tian, F. (2006), Study on thermodynamic watershed hydrological model (THModel), Ph.D. thesis, Department of Hydraulic Engineering, Tsinghua University, Beijing, China, 168 pp.

Tian, F., H. Hu, Z. Lei, and M. Sivapalan (2006), Extension of the representative elementary watershed approach for cold regions via explicit treatment of energy related processes, *Hydrol. Earth Syst. Sci.*, *10*, 619–644.

Viney, N. R., M. Sivapalan, and D. E. Deeley (2000), A conceptual model of nutrient mobilisation and transport applicable at large catchment scales, *J. Hydrol.*, *240*(1–2), 23–44.

Webster, J. R., and B. C. Patten (1979), Effects of watershed perturbation on stream potassium and calcium dynamics, *Ecol. Monogr.*, *49*, 51–72.

Wollheim, W. M., C. J. Vörösmarty, B. J. Peterson, S. P. Seitzinger, and C. S. Hopkinson (2006), Relationship between river size and nutrient removal, *Geophys. Res. Lett.*, *33*, L06410, doi:10.1029/2006GL025845.

Wollheim, W. M., B. J. Peterson, S. M. Thomas, C. H. Hopkinson, and C. J. Vörösmarty (2008), Dynamics of N removal over annual time periods in a suburban river network, *J. Geophys. Res. Biogeosci.*, *113*, G03038.